Sensitivity!initial conditions

Appendix R

Solutions

Chapter 1

Solution 1.1: 3-disk symbolic dynamics. *As explained in sect. 1.4, each orbit segment can be characterized by either of the two symbols* 0 *and* 1*, differentiating topologically bouncing back or going onto the third disk. So, there are* 2^n *topologically different orbits starting from each disk. Altogether, the 3-disk pinball has* $3 \cdot 2^n$ *itineraries of length* n*.*
Periodic orbits (prime cycles in fundamental domain)

- *Of length* 2*: 12,13,32; or (0).*
- *Of length* 3*: 123,321; or (1).*
- *Of length* 4*: 1213,2321,3231; or (01).*
- *Of length* 5*: 12123,13132,23231,21213,32321,31312; or (00111).*

Some of the cycles are listed in table 11.2 and drawn in figure 22.3.

(Yuheng Lan)

Solution 1.2: Sensitivity to initial conditions. *To estimate the pinball sensitivity we consider a narrow beam of point particles bouncing between two disks, figure R.1(a). Or if you find this easier to visualize, think of a narrow ray of light. We*

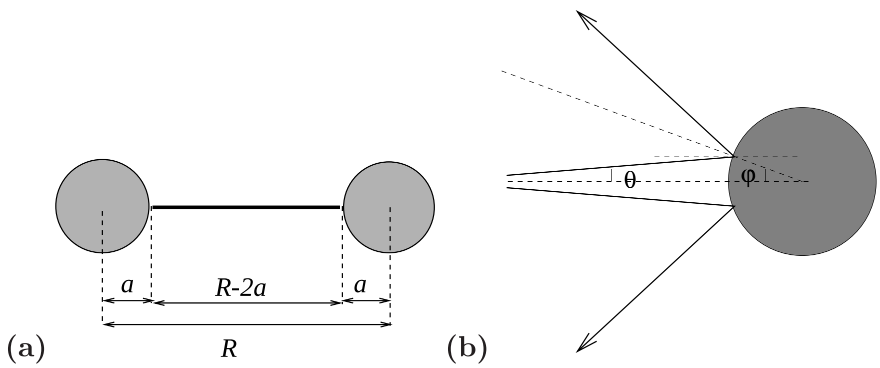

Figure R.1: The 2-disk pinball (a) geometry, (b) defocusing of scattered rays.

assume that the ray of light is focused along the axis between the two points. This is where the least unstable periodic orbit lies, so its stability should give us an upper bound on the number of bounces we can expect to achieve. To estimate the stability we assume that the ray of light has a width $w(t)$ and a "dispersion angle" $\theta(t)$ (we assume both are small), figure R.1(b). Between bounces the dispersion angle stays constant while the width increases as

$$w(t) \approx w(t') + (t - t')\theta$$

At each bounce the width stays constant while the angle increases by

$$\theta_{n+1} = \theta_n + 2\phi \approx \theta_n + w(t)/a.$$

where θ_n denotes the angle after bounce n. Denoting the width of the ray at the nth bounce by w_n then we obtain the pair of coupled equations

$$\begin{aligned} w_{n+1} &= w_n + \left(R - 2a\right)\theta_n && \text{(R.1)} \\ \theta_n &= \theta_{n-1} + \frac{w_n}{a} && \text{(R.2)} \end{aligned}$$

where we ignore corrections of order w_n^2 and θ_n^2. Solving for θ_n we find

$$\theta_n = \theta_0 + \frac{1}{a}\sum_{j=1}^{n} w_n.$$

Assuming $\theta_0 = 0$ then

$$w_{n+1} = w_n + \frac{R - 2a}{a}\sum_{j=1}^{n} w_n$$

Plugging in the values in the question we find the width at each bounce in Ångstrøms grows as 1, 5, 29, 169, 985, etc. To find the asymptotic behavior for a large number of bounces we try an solution of the form $w_n = ax^n$. Substituting this into the equation above and ignoring terms that do not grow exponentially we find solutions

$$w_n \approx a w_n^{asym} = a(3 \pm 2\sqrt{2})^n$$

The solution with the positive sign will clearly dominate. The constant a we cannot determine by this local analysis although it is clearly proportional to w_0. However, the asymptotic solution is a good approximation even for quite a small number of bounces. To find an estimate of a we see that w_n/w_n^{asym} very rapidly converges to 0.146447, thus

$$w_n \approx 0.146447 w_0 (3 + 2\sqrt{2})^n \approx 0.1 \times w_0 \times 5.83^n$$

The outside edges of the ray of light will miss the disk when the width of the ray exceeds 2 cm; this occurs after 11 bounces. evolution!group group!evolution

(Adam Prügel-Bennett)

Solution 1.2: Sensitivity to initial conditions, another try. *Adam's estimate is not very good - do you have a better one? The first problem with it is that the instability is very underestimated. As we shall check in exercise 8.1, the exact formula for the 2-cycle stability is* $\Lambda = R - 1 + R\sqrt{1 - 2/R}$*. For* $R = 6$*,* $a = 1$ *this yields* $w_n/w_0 \approx (5 + 2\sqrt{6})^n = 9.898979^n$*, so if that were the whole story, the pinball would be not likely to make it much beyond 8 bounces.*

The second problem is that local instability overestimates the escape rate from an enclosure; trajectories are reinjected by scatterers. In the 3-disk pinball the particle leaving a disk can be reinjected by hitting either of other 2 disks, hence $w_n/w_0 \approx (9.9/2)^n$*. This interplay between local instability and global reinjection will be cast into the exact formula (Q.1) involving "Lyapunov exponent" and "Kolmogorov entropy". In order to relate this estimate to our best continuous time escape rate estimate* $\gamma = 0.4103\ldots$ *(see table 18.2), we will have to also compute the mean free flight time (18.20). As a crude estimate, we take the shortest disk-to-disk distance,* $\langle T \rangle = R - 2 = 4$*. The continuous time escape rate result implies that* $w_n/w_0 \approx e^{(R-2)\gamma n} = (5.16)^n$*, in the same ballpark as the above expansion-reinjection estimate.* ⇓PRELIMINARY ⇑PRELIMINARY

(Predrag Cvitanović)

Chapter 2

Solution 2.1: Trajectories do not intersect. *Suppose that two trajectories* C_x *and* C_y *intersect at some point* z*. We claim that any points* $\tilde{x}$ *on* C_x *is also a point on* C_y *and vice versa. We only need to prove the first part of the statement. According to the definition of* C_x*, there exist* $t_x, t_y, t_1 \in \mathbb{R}$ *such that* $f^{t_x}(x) = z\,, f^{t_y}(y) = z\,, f^{t_1}(x) = \tilde{x}$*. It is easy to check that* $f^{t_y - t_x + t_1}(y) = \tilde{x}$*. So,* $\tilde{x} \in C_y$*. Therefore, if two trajectories intersect, then they are the same trajectory.*

(Yueheng Lan)

Solution 2.2: Evolution as a group. *Let's check the basic defining properties of a group. The members of the set are* $f^t\,, t \in \mathbb{R}$ *and the "product law" is given by '*$\circ$*'.*

- *As* $f^{t+s} = f^t \circ f^s$*, the set is closed,* i.e., *the product of any two members generates another member of the set.*
- *It is associative, as* $(f^t \circ f^s) \circ f^r = f^{t+s+r} = f^t \circ (f^s \circ f^r)$*.*
- $I = f^0$ *is the identity, as* $f^t \circ f^0 = f^t$*.*
- f^{-t} *is the inverse of* f^t*, as* $f^{-t} \circ f^t = I$*.*

So, $\{f^t, \circ\}_{t \in \mathbb{R}}$ *forms a group. As* $f^t \circ f^s = f^{t+s} = f^s \circ f^t$*, it is a commutative (Abelian) group.*

Any Abelian group can replace the continuous time. For example, $\mathbb{R}$ *can be replaced by* $\mathbb{Z}_6$*. To mess things up try a non-commutative group.*

(Yueheng Lan)

Solution 2.3: Almost ODE's. *What is an ODE on $\mathbb{R}$? An ODE is an equality which reveals explicitly the relation between function $x(t)$ and its time derivatives $\dot{x}, \ddot{x}, \cdots$, i.e., $F(t, x, \dot{x}, \ddot{x}, \cdots) = 0$ for some given function F. Let's check the equations given in the exercise.*
(a) $\dot{x} = \exp(\dot{x})$ is an ODE.
(b) $\dot{x} = x(x(t))$ is not an ODE, as $x(x(t))$ is not a known function acting on $x(t)$.
(c) $\dot{x} = x(t+1)$ is not an ODE, as $x(t+1)$ is not a value at current time. Actually, it is a difference-differential equation.

(Yueheng Lan)

Solution 2.4: All equilibrium points are fixed points. *Given a vector field $v(x)$, the phase space dynamics is defined by*

$$\frac{d}{dt}x(t) = v(x(t)) \,. \tag{R.3}$$

An equilibrium point a of v is defined by $v(a) = 0$, so $x(t) = a$ is a constant solution of (R.3). For the flow f^t defined by (R.3), this solution satisfies $f^t(a) = a\,, t \in \mathbb{R}\,.$ So, it is a fixed point of the dynamics f^t.

(Yueheng Lan)

Solution 2.5: Gradient systems.

1. *The directional derivative*

   $$\frac{d}{dn}\phi = n \cdot \nabla\phi$$

   produces the increasing rate along the unit vector n. So, along the gradient direction $\nabla\phi/|\nabla\phi|$, ϕ has the largest increasing rate. The velocity of the particle has the opposite direction to the gradient, so ϕ deceases most rapidly in the velocity direction.

2. *An extremum a of ϕ satisfies $\nabla\phi(a) = 0$. According to exercise 2.4, a is a fixed point of the flow.*

3. *Two arguments lead to the same conclusion here.*

   First, near an equilibrium point, the equation is always linearizable. For gradient system, after orthogonal transformation it is even possible to write the linearized equation in diagonal form so that we need only to consider one eigendirection. The corresponding scalar equation is $\dot{x} = \lambda x$. Notice that we moved the origin to the equilibrium point. The solution of this equation is $x(t) = x(0)\exp(\lambda t)$, for $\lambda \neq 0$. if $x(0) \neq 0$, it will take infinite amount of time (positive or negative) for $x(t) \to 0$. For $\lambda = 0$, the approach to zero is even slower as then only higher orders of x take effect.

   The second argument seems easier. We know that the solution curve through an equilibrium point is the point itself. According to exercise 2.1, no other solution curve will intersect it, which means that if not starting from the equilibrium point itself, other point can never reach it.

4. *On a periodic orbit, the velocity is bounded away from zero. So ϕ is always decreasing on a periodic orbit, but in view of the periodicity, we know that this can not happen (at each point, there is only one value of ϕ.). So, there is no periodic orbit in a gradient system.*

(Yueheng Lan)

helium!collinear
Rossler@Rössler system!equilibria
equilibrium!Rössler system

Solution 2.11: Classical collinear helium dynamics. *An example of a solution are A. Prügel-Bennett's programs, available at* `ChaosBook.org/extras`.

Solution 2.9: Equilibria of the Rössler system.

1. *Solve* $\dot{x} = \dot{y} = \dot{z} = 0$, *to get* $x = az$, $y = -z$ *and* $x^2 - cx + ab = 0$. *There are two solutions of a quadratic equation, hence there are two equilibrium points:*

$$x^{\pm} = az^{\pm} = -ay^{\pm} = (c \pm \sqrt{c^2 - 4ab})/2\,. \tag{R.4}$$

2. *That above expressions are exact. However, it pays to think of* $\epsilon = a/c$ *as a small parameter in the problem. By subsitution from (2.18),*

$$x^{\pm} = cp^{\pm}, \quad y^{\pm} = -p^{\pm}/\epsilon, \quad z^{\pm} = p^{\pm}/\epsilon. \tag{R.5}$$

Expanding $\sqrt{D}$ *in* ϵ *yields* $p^- = \epsilon^2 + o(\epsilon^3)$, *and* $p^+ = 1 - \epsilon^2 + o(\epsilon^3)$. *Hence*

$$\begin{array}{ll} x^- = a^2/c + o(\epsilon^3), & x^+ = c - a^2/c + o(\epsilon^3), \\ y^- = -a/c + o(\epsilon^2), & z^+ = c/a + a/c + o(\epsilon^2), \\ z^- = a/c + o(\epsilon^2), & z^+ = c/a - a/c + o(\epsilon^2). \end{array} \tag{R.6}$$

For $a = b = 0.2$, $c = 5.7$ *in (2.14),* $\epsilon \approx 0.035$, *so*

$$\begin{array}{l} (x^-, y^-, z^-) = (\,0.0070,\, -0.0351,\, 0.0351\,)\,, \\ (x^+, y^+, z^+) = (\,5.6929,\, -28.464,\, 28.464\,)\,. \end{array} \tag{R.7}$$

(Rytis Paškauskas)

Chapter 3

(No solutions available.)

Chapter 4

Solution 4.1: Trace-log of a matrix. *1) one method is to first check that this is true for any Hermitian matrix* M. *Then write an arbitrary complex matrix as sum* $M = A + zB$, A, B *Hermitian, Taylor expand in* z *and prove by analytic continuation that the identity applies to arbitrary* M. *(David Mermin)*

2) another method: evaluate $\frac{d}{dt}\det\left(e^{t\ln M}\right)$ *by definition of derivative in terms of infinitesimals. (Kasper Juel Eriksen)*

to be fleshed out

3) check appendix M.1

4) This identity makes sense for a matrix $M \subset \mathbb{C}^{n\times n}$, *if* $|\prod_{i=1}^{n} \lambda_i| < \infty$ *and* $\{|\lambda_i| > 0, \forall i\}$, *where* $\{\lambda_i\}$ *is a set of eigenvalues of* M. *Under these conditions there exist a nonsingular* $O : M = ODO^{-1}$, $D = \mathrm{diag}[\{\lambda_i, i = 1, \ldots, n\}]$. *If* $f(M)$ *is a* *matrix valued function defined in terms of power series then* $f(M) = Of(D)O^{-1}$, *and* $f(D) = \mathrm{diag}[\{f(\lambda_i)\}]$. *Using these properties and cyclic property of the trace we obtain*

$$\exp(\mathrm{tr}\,(\ln M)) = \exp\left(\sum_i \ln \lambda_i\right) = \prod_i \lambda_i = \det(M)$$

5) Consider $M = \exp A$.

$$\det M = \det \lim_{n\to\infty}\left(\mathbf{1} + \frac{1}{n}A\right)^n = \lim_{n\to\infty}(\mathbf{1} + \frac{1}{n}\mathrm{tr}\,A + \ldots)^n = \exp(\mathrm{tr}\,(\ln M))$$

Solution 4.2: Stability, diagonal case. *The relation (4.16) can be verified by noting that the defining product (4.11) can be rewritten as*

$$\begin{aligned} e^{t\mathbf{A}} &= \left(\mathbf{U}\mathbf{U}^{-1} + \frac{t\mathbf{U}\mathbf{A}_D\mathbf{U}^{-1}}{m}\right)\left(\mathbf{U}\mathbf{U}^{-1} + \frac{t\mathbf{U}\mathbf{A}_D\mathbf{U}^{-1}}{m}\right)\cdots \\ &= \mathbf{U}\left(I + \frac{t\mathbf{A}_D}{m}\right)\mathbf{U}^{-1}\mathbf{U}\left(I + \frac{t\mathbf{A}_D}{m}\right)\mathbf{U}^{-1}\cdots = \mathbf{U}e^{t\mathbf{A}_D}\mathbf{U}^{-1}\,. \end{aligned} \qquad \text{(R.8)}$$

Solution 4.3: Topology of the Rössler flow.

1. *The characteristic determinant of the matrix of variations that yields the equilibrium point stability (4.25) yields*

   $$\begin{vmatrix} -\lambda & -1 & -1 \\ 1 & a-\lambda & 0 \\ z^{\pm} & 0 & x^{\pm} - c - \lambda \end{vmatrix} = 0$$

   $$\lambda^3 + \lambda^2(-a - x^{\pm} + c) + \lambda(a(x^{\pm} - c) + 1 + x^{\pm}/a) + c - 2x^{\pm} = 0\,.$$

   Equation (4.42) follows after noting that $x^{\pm} - c = c(p^{\pm} - 1) = -cp^{\mp}$ *and* $2x^{\pm} - c = c(2p^{\pm} - 1) = \pm c\sqrt{D}$, *see (2.9).*

2. *Approximate solutions of (4.42) are obtained by expanding* $p^{\pm}$ *and* $\sqrt{D}$ *and substituting into this equation. Namely,*

   $$\begin{aligned} \sqrt{D} &= 1 - 2\epsilon^2 - 2\epsilon^4 - 4\epsilon^6 - \ldots \\ p^- &= \epsilon^2 + \epsilon^4 + 2\epsilon^6 + \ldots \\ p^+ &= 1 - \epsilon^2 - \epsilon^4 - 2\epsilon^6 + \ldots \end{aligned}$$

   In case of the equilibrium "–", close to the origin expansion of (4.42) results in

   $$(\lambda^2 + 1)(\lambda + c) = -\epsilon\lambda(1 - c^2 - c\lambda) + \epsilon^2 c(\lambda^2 + 2) + o(\epsilon^2)$$

   The term on the left-hand side suggests the expansion for eigenvalues as

   $$\lambda_1 = -c + \epsilon a_1 + \ldots\,, \quad \lambda_2 + i\theta_2 = \epsilon b_1 + i + \ldots \quad .$$

   after some algebra one finds the first order correction coefficients $a_1 = c/(c^2+1)$ *and* $b_1 = (c^3 + i)/(2(c^2 + 1))$. *Numerical values are* $\lambda_1 \approx -5.694$, $\lambda_2 + i\theta_2 \approx 0.0970 + i1.0005$.

In case of p^+, the leading order term in (4.42) is $1/\epsilon$. Set $x = \lambda/\epsilon$, then expansion of (4.42) results in

pinball!simulator
billiards
smooth!conjugacy
conjugacy!smooth

$$x = c - \epsilon x - \epsilon^2(2c - x) - \epsilon^3(x^3 - cx^2) - \epsilon^4(2c - x(1 + c^2) + cx^2) + o(\epsilon^4)$$

Solve for real eigenvalue first. Set $x = c + \epsilon a_1 + \epsilon^2 a_2 + \epsilon^3 a_3 + \epsilon^4 a_4 + \ldots$. The subtle point here is that leading order correction term of the real eigenvalue is ϵa_1, but to determine leading order of the real part of complex eigenvalue, one needs all terms a_1 through a_4.

Collecting powers of ϵ results in

$$\begin{array}{lll} \epsilon: & a_1 + c = 0 & a_1 = \ -c \\ \epsilon^2: & c + a_1 + a_2 = 0 & a_2 = \ 0 \\ \epsilon^3: & a_1 - a_2 - a_3 = 0 & a_3 = \ -c \\ \epsilon^4: & c + c^2 a_1 - a_2 + a_3 + a_4 = 0 & a_4 = \ c^3 \,. \end{array}$$

hence

$$\lambda_1 = \epsilon x = a - a^2/c + o(\epsilon^3) \approx 0.192982\,.$$

To calculate the complex eigenvalue, one can make use of identities $\det A = \prod \lambda = 2x^+ - c$*, and* $\operatorname{tr} A = \sum \lambda = a + x^+ - c$*. Namely,*

$$\lambda_2 = \frac{1}{2}\left(a - cp^- - \lambda_1\right) = -\frac{a^5}{2c^2} + o(\epsilon^5) \approx -0.49 \times 10^{-6}\,,$$

$$\theta_2 = \sqrt{\frac{2x^+ - c}{\lambda_1} - \lambda_2^2} = \sqrt{\frac{a+c}{a}}\,(1 + o(\epsilon)) \approx 5.431\,.$$

(Rytis Paškauskas)

Chapter 5

(No solutions available.)

Chapter 6

Solution 6.1: A pinball simulator. *Examples of pretty pinballs are A. Prügel-Bennett's xpinball.c and W. Benfold's java programs, available at* `ChaosBook.org/extras`

Solution 6.4: Billiard exercises. *Korsch and Jodl [1.10] have a whole book of numerical exercises with billiards, including 3-disks.*

Chapter 7

Solution 7.2: Linearization for maps. *(difficulty: medium) The first few terms of the map h that conjugates f to αz*

$$f(z) = h^{-1}(\alpha h(z))\,.$$

are determined many places, for example in ref. [9.5].

coordinate!change
stability!exact
equilibrium!stability
limit cycle!stability

There are conditions on the derivative of f at the origin to assure that the conjugation is always possible. These conditions are formulated in ref. [1.15], among others.

Chapter 8

Solution 8.3: A limit cycle with analytic stability exponent. *The trajectories $x(t) = (q(t), p(t))$ The 2-d flow (8.23) is cooked up so that it is separable (check!) in polar coordinates $q = r\cos\phi\,, \qquad p = r\sin\phi$:*

$$\dot{r} = r(1 - r^2)\,, \qquad \dot{\phi} = 1\,. \tag{R.9}$$

In the (r, ϕ) coordinates the flow starting at any $r > 0$ is attracted to the $r = 1$ limit cycle, with the angular coordinate ϕ wraping around with a constant angular velocity. The non–wandering set of this flow consists of the $r = 0$ equilibrium and the $r = 1$ periodic orbit.

Equilibrium stability. *As the change of coordinates is defined everywhere except at the the equilibrium point ($r = 0$, any ϕ), the equilibrium matrix of variations (4.25) has to be computed in the original (q, p) coordinates,*

$$A = \begin{bmatrix} 1 & 1 \\ -1 & 1 \end{bmatrix}. \tag{R.10}$$

The eigenvalues are $\lambda \pm i\,\theta = 1 \pm i$, indicating that the origin is linearly unstable, with nearby trajectories spiralling out with the constant Poincaré section ($p = 0$, for example) return time $T = 2\pi$, and the radial stability multiplier $\Lambda = e^{2\pi}$ per one Poincaré return.

Limit cycle stability. *From (R.9) the matrix of variations is diagonal in the (r, ϕ) coordinates,*

$$A = \begin{bmatrix} 1 - 3r^2 & 0 \\ 0 & 0 \end{bmatrix}, \tag{R.11}$$

with the $\lambda_\theta = 0$ eigenvalue due to the rotational invariance of the $r = 1$ cycle along ϕ direction, and the radial $\lambda_r = -2$ eigenvalue corresponding to contraction of the radial deviations from $r = 1$ with the radial stability multiplier $\Lambda_r = e^{-4\pi}$ per one Poincaré return. This limit cycle is very *attracting.*

Stability of a trajectory segment. *Multiply (R.9) by r to obtain $\frac{1}{2}\dot{\overline{r^2}} = r^2 - r^4$, separate variables*

$$\frac{dr^2}{r^2(1-r^2)} = \frac{dr^2}{r^2} + \frac{dr^2}{1-r^2} = 2\,dt\,,$$

and integrate

$$\frac{r^2}{1-r^2} = \frac{r_0^2}{1-r_0^2}e^{2t}\,.$$

After a bit of algebra one gets the $r(r_0, t)$ trajectory

Dirac delta function
delta function!Dirac

$$r(t)^2 = \frac{r_0^2}{r_0^2 + (1 - r_0^2)e^{-2t}} . \tag{R.12}$$

The $[1\times1]$ Jacobian matrix

$$J(r_0, t) = \left. \frac{\partial r(t)}{\partial r_0} \right|_{r_0 = r(0)} . \tag{R.13}$$

satisfies (4.32)

$$\frac{d}{dt} J(r, t) = A(r)\, J(r, t) = (1 - 3r(t)^2)\, J(r, t) , \qquad J(r_0, 0) = 1 .$$

This too can be integrated by separating variables $d(\ln J(r, t)) = dt - 3r(t)^2 dt$, substituting (R.14) and integrating. The stability of a finite trajectory segment is:

$$J(r_0, t) = \frac{1}{(r_0^2 + (1 - r_0^2)e^{-2t})^{3/2}} e^{-2t} . \tag{R.14}$$

This general formula agrees with the limit cycle contraction $\Lambda_r(1, t) = e^{-2t}$ when $r = 1$, and with the radial part of the equilibrium instability $\Lambda_r(r_0, t) = e^t$ for $r_0 \ll 1$.

P. Cvitanović

Chapter 9

Solution 9.1: Integrating over Dirac delta functions. (a) Whenever $h(x)$ crosses 0 with a nonzero velocity ($\det \partial_x h(x) \neq 0$), the delta function contributes to the integral. Let $x_0 \in h^{-1}(0)$. Consider a small neighborhood V_0 of x_0 so that $h : V_0 \to V_0$ is a one-to-one map, with the inverse function $x = x(h)$. By changing variable from x to h, we have

$$\begin{aligned} \int_{V_0} dx\, \delta(h(x)) &= \int_{h(V_0)} dh\, |\det \partial_h x|\, \delta(h) = \int_{h(V_0)} dh\, \frac{1}{|\det \partial_x h|} \delta(h) \\ &= \frac{1}{|\det \partial_x h|_{h=0}} . \end{aligned}$$

Here, the absolute value $|\cdot|$ is taken because delta function is always positive and we keep the orientation of the volume when the change of variables is made. Therefore all the contributions from each point in $h^{-1}(0)$ add up to the integral

$$\int_{\mathbb{R}^d} dx\, \delta(h(x)) = \Sigma_{x \in h^{-1}(0)} \frac{1}{|\det \partial_x h|} .$$

Notice that if $\det \partial_x h = 0$, then the delta function integral is not well defined.

(b) The formal expression can be written as the limit

$$F := \int_{\mathbb{R}} dx\, \delta(x^2) = \lim_{\sigma\to 0} \int_{\mathbb{R}} dx\, \frac{e^{-\frac{x^4}{2\sigma}}}{\sqrt{2\pi\sigma}}\,,$$

by invoking the approximation given in the exercise. The change of variable $y = x^2/\sqrt{\sigma}$ *gives*

$$F = \lim_{\sigma\to 0} \sigma^{-3/4} \int_{\mathbb{R}^+} dy\, \frac{e^{-\frac{y^2}{2}}}{\sqrt{2\pi y}} = \infty\,,$$

where $\mathbb{R}^+$ *represents the positive part of the real axis. So, the formal expression does not make sense. Notice that* x^2 *has a zero derivative at* $x = 0$*, which invalidates the expression in (a).*

(Yueheng Lan)

Solution 9.2: Derivatives of Dirac delta functions. *We do this problem just by direct evaluation. We denote by* Ω_y *a sufficiently small neighborhood of* y*.*
(a)

$$\begin{aligned}
\int_{\mathbb{R}} dx\, \delta'(y) &= \Sigma_{x\in y^{-1}(0)} \int_{\Omega_y} dy\, \det\,(\frac{dy}{dx})^{-1}\delta'(y) \\
&= \Sigma_{x\in y^{-1}(0)} \frac{\delta(y)}{|y'|}|_{-\epsilon}^{\epsilon} - \int_{\Omega_y} dy\, \frac{\delta(y)}{y'^2}(-y'')\frac{1}{y'} \\
&= \Sigma_{x\in y^{-1}(0)} \frac{y''}{|y'|y'^2}\,,
\end{aligned}$$

where the absolute value is taken to take care of the sign of the volume.

(b)

$$\begin{aligned}
\int_{\mathbb{R}} dx\, \delta^{(2)}(y) &= \Sigma_{x\in y^{-1}(0)} \int_{\Omega_y} dy\, \frac{\delta^{(2)}(y)}{y'} \\
&= \Sigma_{x\in y^{-1}(0)} \frac{\delta'(y)}{|y'|}|_{-\epsilon}^{\epsilon} - \int_{\Omega_y} dy\, \frac{\delta'(y)}{y'^2}(-y'')\frac{1}{y'} \\
&= \Sigma_{x\in y^{-1}(0)} \frac{y''\delta(y)}{|y'|y'^2}|_{-\epsilon}^{\epsilon} - \int_{\Omega_y} dy\, \delta(y)\frac{d}{dx}(\frac{y''}{y'^3})\frac{1}{y'} \\
&= \Sigma_{x\in y^{-1}(0)} - \int_{\Omega_y} dy\, \delta(y) \left(\frac{y'''}{y'^3} - 3\frac{y''^2}{y'^4}\right)\frac{1}{y'} \\
&= \Sigma_{x\in y^{-1}(0)} \left(3\frac{y''^2}{y'^4} - \frac{y'''}{y'^3}\right)\frac{1}{|y'|}\,.
\end{aligned}$$

(c)

$$\int_{\mathbb{R}} dx\, b(x)\delta^{(2)}(y) = \Sigma_{x\in y^{-1}(0)} \int_{\Omega_y} dy\, b(x)\frac{\delta^{(2)}(y)}{y'}$$

$$
\begin{aligned}
&= \Sigma_{x\in y^{-1}(0)} \frac{b(x)\delta'(y)}{|y'|}|_{-\epsilon}^{\epsilon} - \int_{\Omega_y} dy\, \delta'(y) \frac{d}{dx}(\frac{b}{y'})\frac{1}{y'} \\
&= \Sigma_{x\in y^{-1}(0)} - \delta(y)\frac{d}{dx}(\frac{b}{y'})\frac{1}{y'}|_{-\epsilon}^{\epsilon} + \int_{\Omega_y} dy\, \delta(y)\frac{d}{dx}(\frac{d}{dx}(\frac{b}{y'})\frac{1}{y'})\frac{1}{y'} \\
&= \Sigma_{x\in y^{-1}(0)} \frac{1}{|y'|}\frac{d}{dx}(\frac{b'}{y'^2} - \frac{by''}{y'^3})) \\
&= \Sigma_{x\in y^{-1}(0)} \frac{1}{|y'|}\left[\frac{b''}{y'^2} - \frac{b'y''}{y'^3} - 2\frac{b'y''}{y'^3} + b(3\frac{y''^2}{y'^4} - \frac{y'''}{y'^3})\right] \\
&= \Sigma_{x\in y^{-1}(0)} \frac{1}{|y'|}\left[\frac{b''}{y'^2} - 3\frac{b'y''}{y'^3} + b(3\frac{y''^2}{y'^4} - \frac{y'''}{y'^3})\right] .
\end{aligned}
$$

(Yueheng Lan)

Solution 9.3: $\mathcal{L}^t$ generates a semigroup. *Every "sufficiently good" transformation f^t in phase space $\mathcal{M}$ is associated with a Perron-Frobenius operator $\mathcal{L}^t$ which is when acting on a function $\rho(x)$ in $\mathcal{M}$*

$$
\mathcal{L}^t \cdot \rho(x) = \int_{\mathcal{M}} dy\, \delta(x - f^t(y))\rho(y) .
$$

In some proper function space $\mathcal{F}$ on $\mathcal{M}$, the one parameter family of operators $\{\mathcal{L}^t\}_{t\in\mathbb{R}^+}$ generate a semigroup. Let's check this statement. For any $t_1, t_2 > 0$ and $\rho \in \mathcal{F}$, the product "$\circ$" of two operators is defined as usual

$$
(\mathcal{L}^{t_1} \circ \mathcal{L}^{t_2}) \cdot \rho(y) = \mathcal{L}^{t_1} \cdot (\mathcal{L}^{t_2} \cdot \rho)(y) .
$$

So, we have

$$
\begin{aligned}
(\mathcal{L}^{t_1} \circ \mathcal{L}^{t_2})(y,x) &= \int_{\mathcal{M}} dz\, \mathcal{L}^{t_1}(y,z)\mathcal{L}^{t_2}(z,x) \\
&= \int_{\mathcal{M}} dz\, \delta(y - f^{t_1}(z))\delta(z - f^{t_2}(x)) \\
&= \delta(y - f^{t_1}(f^{t_2}(x))) \\
&= \delta(y - f^{t_1+t_2}(x)) \\
&= \mathcal{L}^{t_1+t_2}(y,x) ,
\end{aligned}
$$

where the semigroup property $f^{t_1}(f^{t_2}(x)) = f^{t_1+t_2}(x)$ of f^t has been used. This proves the claim in the title.

(Yueheng Lan)

Solution 9.5: Invariant measure. *Hint: Compare the second map to the construction of Exercise 13.6. We do (a),(b),(c),(d) for the first map and (e) for the second.*
(a) The partition point is in the middle of $[0,1]$. If the density on the two pieces are two constants ρ_0^A and ρ_0^B, respectively, the Perron-Frobenius operator still leads to the piecewise constant density

$$
\rho_1^A = \frac{1}{2}(\rho_0^A + \rho_0^B) ,
$$
$$
\rho_1^B = \frac{1}{2}(\rho_0^A + \rho_0^B) .
$$

Notice that in general if a finite Markov partition exists and the map is affine (linear on each partition cell), a finite-dimensional invariant subspace consisting of piecewise constant function can always be identified in the function space.

(b) From the discussion of (a), any constant function on $[0,1]$ *is an invariant measure. If we consider the invariant probability measure, then the constant has to be* 1.

(c) As the map is invariant in $[0,1]$ *(there is no escaping), the leading eigenvalue of* $\mathcal{L}$ *is always 1 due to the "mass" conservation.*

(d) Take a typical point on $[0,1]$ *and record its trajectory under the first map for some time (*10^5 *steps). Plot the histogram...ONLY* 0 *is left finally!! This happens because of the finite accuracy of the computer arithmetics. A small trick is to change the slope* 2 *to* 1.99999999*. You will find a constant measure on* $[0,1]$ *which is the natural measure. Still, the finite presicion of the computer will make every point eventually periodic and strictly speaking the measure is defined only on some fine lattice points. But when the resolution improves, the computer-generated measure will steadily approach the natural measue. For the first map, any small deviation from the constant profile will be stretched and smeared out. So, the natural measure has to be constant.*

(e) Simple calculation shows that α *is the partition point. We may use* $A\,,B$ *to mark the left and right part of the partition, respectively.* A *maps to* B *and* B *maps to the whole interval* $[0,1]$*. As the magnitude of the slope* $\Lambda=(\sqrt{5}+1)/2$ *is greater than* 1*, we may expect the natural measure is still piecewise constant with eigenvalue* 1*. The determining equation is*

$$\left(\begin{array}{cc} 0 & 1/\Lambda \\ 1/\Lambda & 1/\Lambda \end{array}\right)\left(\begin{array}{c} \rho^A \\ \rho^B \end{array}\right)=\left(\begin{array}{c} \rho^A \\ \rho^B \end{array}\right),$$

which gives $\rho^B/\rho^A=\Lambda$.

(Yueheng Lan)

Solution 9.7: Eigenvalues of the skew Ulam tent map Perron-Frobenius operator. *If we have density* $\rho_n(x)$*, the action of the Perron-Frobenius operator associated with* $f(x)$ *gives a new density*

$$\rho_{n+1}(x)=\frac{1}{\Lambda_0}\rho_n(x/\Lambda_0)+\frac{1}{\Lambda_1}\rho_n(1-x/\Lambda_1)\,,$$

where $\Lambda_1=\frac{\Lambda_0}{\Lambda_0-1}$*. The eigenvalue equation is given by*

$$\rho_{n+1}(x)=\lambda\rho_n(x)\,. \tag{R.15}$$

We may solve it by assuming that the eigenfunctions are N*-th order polynomials* $P(N)$ *(check it). Indeed, detailed calculation gives the following results:*

- $P(0)$ *gives* $\lambda=1$*, corresponding to the expected leading eigenvalue.*

- *$P(1)$ gives $\lambda = \frac{1}{\Lambda_0^2} - \frac{1}{\Lambda_1^2} = \frac{2}{\Lambda_0} - 1$,*
- *$P(2)$ gives $\lambda = \frac{1}{\Lambda_0^3} + \frac{1}{\Lambda_1^3}$,*
- *$P(3)$ gives $\lambda = \frac{1}{\Lambda_0^4} - \frac{1}{\Lambda_1^4}$,*
- *The guess is that $P(N)$ gives $\lambda = \frac{1}{\Lambda_0^{N+1}} + (-1)^N \frac{1}{\Lambda_1^{N+1}}$.*

Henon@Hénon!attractor!Lyapunov exponent

The final solution is that the piecewise linear function $\rho^A = -\Lambda_0\,, \rho^B = \Lambda_1$ gives the eigenvalue 0. If only the continuous functions are considered, this kind of eigenfunction of course should not be included.

(Yueheng Lan)

Solution 9.7: Eigenvalues of the skew Ulam tent map Perron-Frobenius operator. *The first few eigenvalues are*

$$
\begin{aligned}
e^{s_0} &= 1\,, \qquad e^{s_1} = \frac{2}{\Lambda_0} - 1 \\
e^{s_2} &= \frac{1}{4} + \frac{3}{4}\left(\frac{2}{\Lambda_0} - 1\right)^2, \qquad e^{s_3} = \frac{1}{2}\left(\frac{2}{\Lambda_0} - 1\right) + \frac{1}{2}\left(\frac{2}{\Lambda_0} - 1\right)^3 \ldots
\end{aligned}
$$

For eigenvectors (invariant densities for skew tent maps), see for example Invariant densities for skew tent maps by L. Billings and E.M. Bolt.

Solution 9.10: $\mathcal{A}$ as a generator of translations. *If v is a constant in space, Taylor series expansion gives*

$$
a(x+tv) = \Sigma_{k=0}^{\infty} \frac{1}{k!}(tv\frac{\partial}{\partial x})^k a(x) = e^{tv\frac{\partial}{\partial x}} a(x)\,.
$$

(Yueheng Lan)

Chapter 10

Solution 10.1: How unstable is the Hénon attractor?

1. *Evaluate numerically the Lyapunov exponent by iterating the Hénon map; For $a = 1.4$, $b = 0.3$ the answer should be close to $\lambda = 0.41$. If you have a good estimate and a plot of the convergence of your estimate with t, please send us your results for possible inclusion into this text.*

   Insert here our best estimates, or Grassberger's.

2. *Both Lyapunov exponents for $a = 1.39945219$, $b = 0.3$ are negative, roughly $\lambda_1 = -0.2712, \lambda_2 = -0.9328$ (check that these values respect the constant volume contraction condition (4.37) for the Hénon map). Why? Because after a long transient exploration of the Hénon map's non–wandering set, on average after some 11,000 iterates, almost every inital point falls into a stable 13-cycle. You can check its existence by starting at one of its periodic points $(x_p, y_p) = (-0.2061, -0.3181)$.*

   If you missed the stable 13-cycle (as all students in one of the courses did), you should treat your computer experiments with great deal of scepticism.

As the product of eigenvalues is the constant $-b$, you need to evaluate only the expanding eigenvalue. There are many ways to implement this calculation - here are a few:

1. *The most naive way - take the log of distance of two nearby trajectories, iterate until you run out of accuracy. Tray this many times, estimate an average.*
2. *Slighly smarter: as above, but keep rescaling the length of the vector connecting neighboring points so it remains small, average over the sum of logs of rescaling factors. You can run this forever.*
3. *Keep multiplying the [2×2] Jacobian stability matrix (4.36) until you run out of accuracy. Compute the log of the leading eigenvalue (4.18), try this many times, estimate an average.*
4. *Slighly smarter still: as above, but start with an arbitrary initial tangent space vector, keep multiplying it with the Jacobian stability matrix, and rescaling the length of the vector so it remains small. You can run this forever.*
5. *There is probably no need to use the QR decomposition method or any other such numerical method for this 2-dimensional problem.*

(Yueheng Lan and P. Cvitanović)

Chapter 11

Solution 11.1: Binary symbolic dynamics. *Read the text.*

Solution 11.2: 3-disk fundamental domain symbolic dynamics. *Read sect. 1.4.*

Solution 11.5: Reduction of 3-disk symbolic dynamics. *The answer is given in sect. 22.6. Some remarks concerning part (c):*

If an orbit does not have any spatial symmetry, its length in the fundamental domain is equal to that in the full space. One fundamental domain orbit corresponds to six copies of the orbit in the full space related to each other by symmetries. If a periodic orbit does have a spatial symmetry, then its fundamental domain image is a fraction of that in the whole space, and the orbit (and its symmetry pratnenrs) in the full space is tiled by copies of the irreducible segment, corresponding to an orbit in the fundamental domain. The higher symmetry an orbit has, the shorter the irreducible segment.

Another way to construct a fundamental domain orbit: put a periodic orbit and all its spatial symmetry relatives simultaneously in the full space. The segments that fall into a fundamental domain constitute the orbit in the fundamental domain.

(Yueheng Lan)

Solution 11.6: Unimodal map symbolic dynamics. *Hint: write down an arbitrary binary number such as $\gamma = .1101001101000\ldots$ and generate the future itinerary S^+ by checking whether $f^n(\gamma)$ is greater or less than 1/2. Then verify that (**??**) recovers γ.*

Solution 11.8: "Golden mean" pruned map.
(a) Consider the 3-cycle drawn in the figure. Denote the lengths of the two horizontal intervals by a and b. We have

$$\frac{a}{b} = \frac{b}{a+b},$$

so the slope is given by the golden mean, $\Lambda = \frac{b}{a} = \frac{1+\sqrt{5}}{2}$, and the piece-wise linear map is given by

$$f(x) = \begin{cases} \Lambda x\,,\ x \in [0,1/2] \\ \Lambda(1-x)\,,\ x \in [1/2,1] \end{cases}$$

(b) Evaluate

$$f\left(\frac{1}{2}\right) = \frac{1+\sqrt{5}}{4}, \quad f\left(\frac{1+\sqrt{5}}{4}\right) = \frac{-1+\sqrt{5}}{4}, \quad f\left(\frac{-1+\sqrt{5}}{4}\right) = \frac{1}{2}.$$

Once a point enters the region covered by the interval $\mathcal{M}$ of length $a+b$, bracketed by the 3-cycle, it will be trapped there forever. Outside $\mathcal{M}$, all points on unit interval will be mapped to $(0,1/2]$, except for 0. The points in the interval $(0, \frac{-1+\sqrt{5}}{4})$ approach $\mathcal{M}$ monotonically.

(c) It will be in $(\frac{1}{2}, \frac{1+\sqrt{5}}{4})$.

(d) From (b), we know that except for the origin 0, all periodic orbits should be in $\mathcal{M}$. By (c), we cannot have the substring 00 in a periodic orbit (except for the fixed point at 0). Hence 00 is the only pruning block, *and the symbolic dynamics is a finite subshift, with alphabet $\{0,1\}$ and only one grammar rule: a consecutive repeat of symbol 0 is inadmissible.*

(e) Yes. 0 is a periodic orbit with the symbol sequence $\overline{0}$. It is a repeller and no point in its neighborhood will return. So it plays no role in the asymptotic dynamics.

(Yueheng Lan)

Chapter 12

(No solutions available.)

Chapter 13

Solution 13.1: A transition matrix for 3-disk pinball. *a) As the disk is convex, the transition to itself is forbidden. Therefore, the Markov diagram is*

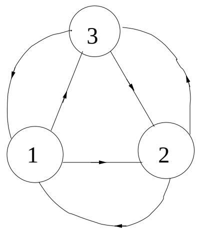

,

with the corresponding transition matrix

$$\mathbb{T} = \begin{pmatrix} 0 & 1 & 1 \\ 1 & 0 & 1 \\ 1 & 1 & 0 \end{pmatrix} .$$

Note that $\mathbb{T}^2 = \mathbb{T} + 2$. *Suppose that* $\mathbb{T}^n = a_n \mathbb{T} + b_n$, *then*

$$\mathbb{T}^{n+1} = a_n \mathbb{T}^2 + b_n \mathbb{T} = (a_n + b_n)\mathbb{T} + 2a_n .$$

So $a_{n+1} = a_n + b_n\,,\ b_{n+1} = 2a_n$ *with* $a_1 = 1\,,\ b_1 = 0$.

b) From a) we have $a_{n+1} = a_n + 2a_{n-1}$. *Suppose that* $a_n \propto \lambda^n$. *Then* $\lambda^2 = \lambda + 2$. *Solving this equation and using the initial condition for* $n = 1$, *we obtain the general formula*

$$\begin{aligned} a_n &= \frac{1}{3}(2^n - (-1)^n)\,, \\ b_n &= \frac{2}{3}(2^{n-1} + (-1)^n)\,. \end{aligned}$$

c) $\mathbb{T}$ *has eigenvalue* 2 *and* -1 *(degeneracy* 2*). So the topological entropy is* $\ln 2$, *the same as in the case of the binary symbolic dynamics.* *(Yueheng Lan)*

Solution 13.2: Sum of A_{ij} is like a trace. *Suppose that* $A\phi_k = \lambda_k\phi_k$, *where* $\lambda_k\,,\phi_k$ *are eigenvalues and eigenvectors, respectively. Expressing the vector* $v = (1, 1, \cdots, 1)^t$ *in terms of the eigenvectors* ϕ_k, *that is,* $v = \Sigma_k d_k\phi_k$, *we have*

$$\begin{aligned} \Gamma_n &= \Sigma_{ij}[A^n]_{ij} = v^t A^n v \ = \Sigma_k v^t A^n d_k\phi_k \ = \Sigma_k d_k \lambda_k^n (v^t\phi_k) \\ &= \Sigma_k c_k \lambda_k^n\,, \end{aligned}$$

where $c_k = (v^t\phi_k)d_k$ *are constants.*

a) As $\mathrm{tr}\, A^n = \Sigma_k\lambda_k^n$, *it is easy to see that both* $\mathrm{tr}\, A^n$ *and* Γ_n *are dominated by the largest eigenvalue* λ_0. *That is*

$$\frac{\ln|\mathrm{tr}\, A^n|}{\ln|\Gamma_n|} = \frac{n\ln|\lambda_0| + \ln|\Sigma_k(\frac{\lambda_k}{\lambda_0})^n|}{n\ln|\lambda_0| + \ln|\Sigma_k d_k(\frac{\lambda_k}{\lambda_0})^n|} \to 1 \ \text{ as } n \to \infty\,.$$

b) The nonleading eigenvalues do not need to be distinct, as the ratio in a) is controlled by the largest eigenvalues only.

(Yueheng Lan)

Solution 13.4: Transition matrix and cycle counting. *a) According to the definition of* $\mathbb{T}_{ij}$, *the transition matrix is*

$$\mathbb{T} = \begin{pmatrix} a & c \\ b & 0 \end{pmatrix} .$$

b) All walks of length three $0000, 0001, 0010, 0100, 0101, 1000, 1001, 1010$ *(four symbols!) with weights* $aaa, aac, acb, cba, cbc, baa, bac, bcb$ *. Let's calculate* $\mathbb{T}^3$*,*

$$\mathbb{T}^3 = \left(\begin{array}{ll} a^3 + 2abc & a^2c + bc^2 \\ a^2b + b^2c & abc \end{array} \right) .$$

There are altogether 8 *terms, corresponding exactly to the terms in all the walks.*

c) Let's look at the following equality

$$\mathbb{T}^n_{ij} = \Sigma_{k_1,k_2,\cdots,k_{n-1}} \mathbb{T}_{ik_1} \mathbb{T}_{k_1k_2} \cdots \mathbb{T}_{k_{n-1}j} .$$

Every term in the sum is a possible path from i *to* j*, though the weight could be zero. The summation is over all possible intermediate points (*$n-1$ *of them). So,* $\mathbb{T}^n_{ij}$ *gives the total weight (probability or number) of all the walks from* i *to* j *in n steps.*

d) We take $a = b = c = 1$ *to just count the number of possible walks in* n *steps. This is the crudest description of the dynamics. Taking* a, b, c *as transition probabilities would give a more detailed description. The eigenvlues of* $\mathbb{T}$ *is* $(1 \pm \sqrt{5})/2$*, so we get* $N(n) \propto (\frac{1+\sqrt{5}}{2})^n$*.*

e) The topological entropy is then $\ln \frac{1+\sqrt{5}}{2}$*.* *(Yueheng Lan)*

Solution 13.6: "Golden mean" pruned map. *It is easy to write the transition matrix* $\mathbb{T}$

$$\mathbb{T} = \left(\begin{array}{ll} 0 & 1 \\ 1 & 1 \end{array} \right) .$$

The eigenvalues are $(1 \pm \sqrt{5})/2$*. The number of periodic orbits of length* n *is the trace*

$$\mathbb{T}^n = \frac{(1+\sqrt{5})^n + (1-\sqrt{5})^n}{2^n} .$$

(Yueheng Lan)

Solution 13.5: 3-disk prime cycle counting. *The formula for arbitrary length cycles is derived in sect. 13.4.*

Solution 13.45: Alphabet $\{$**0,1**$\}$**, prune** $\_1000\_$**,** $\_00100\_$**,** $\_01100\_$**.**

step 1. $\_1000\_$ *prunes all cycles with a* $\_000\_$ *subsequence with the exception of the fixed point* $\overline{0}$*; hence we factor out* $(1 - t_0)$ *explicitly, and prune* $\_000\_$ *from the rest. Physically this means that* x_0 *is an isolated fixed point - no cycle stays in its vicinity for more than 2 iterations. In the notation of exercise 13.19, the alphabet is* $\{$*1, 2, 3;* $\overline{0}\}$*, and the remaining pruning rules have to be rewritten in terms of symbols 2=10, 3=100:*

step 2. *alphabet* $\{$*1, 2, 3;* $\overline{0}\}$*, prune* $\_33\_$*,* $\_213\_$*,*$\_313\_$*. Physically, the 3-cycle* $\overline{3} = \overline{100}$ *is pruned and no long cycles stay close enough to it for a single* $\_100\_$ *repeat.*

As in exercise 13.7, prohibition of $\_33\_$ *is implemented by dropping the symbol "3" and extending the alphabet by the allowed blocks 13, 23:*

step 3. *alphabet* $\{1, 2, \underline{13}, \underline{23}; \overline{0}\}$*, prune* $\_2\underline{13}\_$, $\_\underline{23}\,\underline{13}\_$, $\_\underline{13}\,\underline{13}\_$*, where* $\underline{13} = 13$, $\underline{23} = 23$ *are now used as single letters. Pruning of the repetitions* $\_\underline{13}\,\underline{13}\_$ *(the 4-cycle* $\overline{13} = \overline{1100}$ *is pruned) yields the*

Result: *alphabet* $\{1, 2, \underline{23}, \underline{113}; \overline{0}\}$*, unrestricted 4-ary dynamics. The other remaining possible blocks* $\_\underline{213}\_$, $\_\underline{2313}\_$ *are forbidden by the rules of step 3. The topological zeta function is given by*

$$1/\zeta = (1 - t_0)(1 - t_1 - t_2 - t_{23} - t_{113}) \tag{R.16}$$

for unrestricted 4-letter alphabet $\{1, 2, \underline{23}, \underline{113}\}$.

Solution 13.8: Spectrum of the "golden mean" pruned map.

1. *The idea is that with the redefinition* $2 = 10$*, the alphabet {1,2} is unrestricted binary, and due to the piecewise linearity of the map, the stability weights factor in a way similar to (14.10).*
2. *As in (15.10), the spectral determinant for the Perron-Frobenius operator takes form (15.12)*

$$\det(1 - z\mathcal{L}) = \prod_{k=0}^{\infty} \frac{1}{\zeta_k}, \qquad \frac{1}{\zeta_k} = \prod_p \left(1 - \frac{z^{n_p}}{|\Lambda_p|\Lambda_p^k}\right).$$

The mapping is piecewise linear, so the form of the topological zeta function worked out in (13.16) already suggests the form of the answer. The alphabet {1,2} is unrestricted binary, so the dynamical zeta functions receive contributions only from the two fixed points, with all other cycle contributions cancelled exactly. The $1/\zeta_0$ *is the spectral determinant for the transfer operator like the one in (10.19) with the* $T_{00} = 0$*, and in general*

$$\begin{aligned} \frac{1}{\zeta_k} &= \left(1 - \frac{z}{|\Lambda_1|\Lambda_1^k}\right)\left(1 - \frac{z^2}{|\Lambda_2|\Lambda_2^k}\right)\left(1 - \frac{z^3}{|\Lambda_{12}|\Lambda_{12}^k}\right)\cdots \\ &= 1 - (-1)^k\left(\frac{z}{\Lambda^{k+1}} + \frac{z^2}{\Lambda^{2k+2}}\right). \end{aligned} \tag{R.17}$$

The factor $(-1)^k$ *arises because both stabilities* Λ_1 *and* Λ_2 *include a factor* $-\Lambda$ *from the right branch of the map.*

Solution 15.2: Dynamical zeta functions

1. *Work through section sect. 15.3.2.*
2. *Generalize the transition matrix (11.15) to a transfer operator.*

Solution 13.12: Whence Möbius function? *Written out* $f(n)$ *line-by-line for a few values of* n*, (13.38) yields*

$$\begin{aligned} f(1) &= g(1) \\ f(2) &= g(2) + g(1) \end{aligned}$$

$$\begin{aligned} f(3) &= g(3)+g(1) \\ f(4) &= g(4)+g(2)+g(1) \\ &\cdots \\ f(6) &= g(6)+g(3)+g(2)+g(1) \\ &\cdots \end{aligned} \tag{R.18}$$

Now invert recursively this infinite tower of equations to obtain

$$\begin{aligned} g(1) &= f(1) \\ g(2) &= f(2)-f(1) \\ g(3) &= f(3)-f(1) \\ g(4) &= f(4)-[f(2)-f(1)]-f(1)=f(4)-f(2) \\ &\cdots \\ g(6) &= f(6)-[f(3)-f(1)]-[f(2)-f(1)]-f(1) \\ &\cdots \end{aligned}$$

We see that $f(n)$ contributes with factor -1 if n prime, and not at all if n contains a prime factor to a higher power. This is precisely the raison d'etre for the Möbius function, with whose help the inverse of (13.38) can be written as the Möbius inversion formula [25.29] (13.39).

Chapter 14

(No solutions available.)

Chapter 15

Solution 15.1: Numerical estimate of the escape rate for a 1-d repeller *The logistic map is defined by $x_{n+1} = Ax_n(1-x_n)$. For $A \leq 4$ any point in the unit interval $[0,1]$ will remain in the interval forever. For $A > 4$ almost all points starting in the unit interval will eventually escape towards $-\infty$.*

The rate of escape can be easily measured by numerical experiment. We define the fraction of initial conditions that leave the interval after n iterations to be Γ_n. Figure R.2 shows a plot of $\log(\Gamma_n)$ versus n, computed by starting with $10\,000\,000$ random initial points. Asymptotically the escape rate falls off exponentially as

$$\Gamma(n) = C\mathrm{e}^{-\gamma n}\,.$$

Figure R.2 suggests that this formula is very accurate even for relatively small n. We estimate γ by measuring the slope of the curve in figure R.2. To avoid errors due to rounding and transients only the points $5 \leq n \leq 10$ were used. A linear regression fit yields the escape rate for $A = 6$:

$$\gamma = 0.8315 \pm 0.0001\,,$$

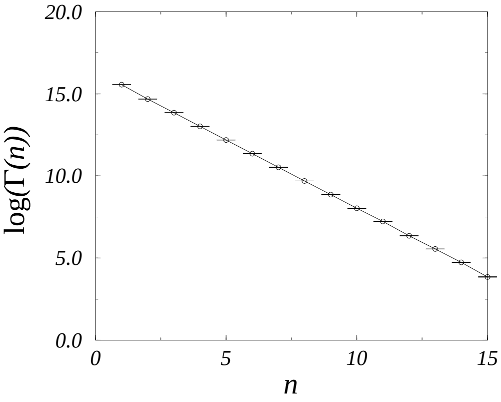

Figure R.2: Plot of $\log(\Gamma(n))$ versus n for the logistic map $x_{n+1} = 6x_n(1 - x_n)$. Error bars show estimated errors in the mean assuming a binomial distribution. $10\,000\,000$ random initial starting points were used.

where the error is from statistical fluctuations (there may be systematic errors either due to rounding or because we are not in the true asymptotic regime).

(Adam Prügel-Bennet)

Solution 15.2: Dynamical zeta functions

1. *Work through section sect. 15.3.2.*
2. *Generalize the transition matrix (11.15) to a transfer operator.*

Solution 15.5: Dynamical zeta functions as ratios of spectral determinants. *Try inserting a factor equal to one in the zeta function and then expanding it. The problem is solved in sect. 15.5.*

Solution 15.8: Dynamical zeta functions for Hamiltonian maps. *Read sect. 15.8.*

Chapter 16

Solution 16.3: Euler formula. *Let*

$$P = \prod_{k=0}^{\infty}(1 + tu^k) = \sum_{n=0}^{\infty} P_n t^n$$

then

$$\begin{aligned} P_n &= \frac{1}{n!}\left.\frac{\partial^n P}{\partial t^n}\right|_{t=0} = \frac{1}{n!}\sum_{i_n \neq i_{n-1} \neq \cdots \neq i_1} u^{i_n + i_{n-1} + \cdots + i_1} \\ &= \sum_{i_n > i_{n-1} > \cdots i_1 \geq 0} u^{i_n + i_{n-1} + \cdots + i_1} \end{aligned} \tag{R.19}$$

Clearly $P_0 = 1$*, and*

$$P_1 = \sum_{i=0} u^i$$

multiplying both sides by $1-u$

$$(1-u)P_1 = 1 + u + u^2 + \cdots - (u + u^2 + \cdots) = 1$$

(since, for $|u| < 1$, $\lim_{n\to\infty} u^n = 0$*). Thus* $P_1 = 1/(1-u)$*. Similarly*

$$P_2 = \sum_{i>j\geq 0} u^{i+j}$$

Graphically the allowed values of i *and* j *are*

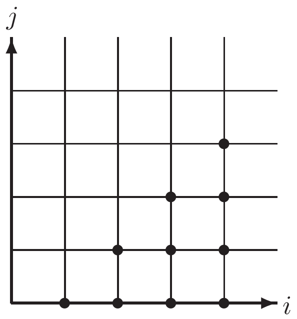

Performing the same trick as for P_1

$$(1-u)P_2 = \sum_{i>j\geq 0} u^{i+j} - \sum_{i>j\geq 0} u^{i+(j+1)}$$

The only terms that survive are those for which $j = i - 1$ *(that is the top diagonal in the figure) thus*

$$(1-u)P_2 = u^{-1}\sum_{i=1}^{\infty} u^{2i}$$

and

$$(1-u)(1-u^2)P_2 = u^{-1}\left(u^2 + u^4 + \cdots - (u^4 + u^6 + \cdots)\right) = u$$

Thus

$$P_2 = \frac{u}{(1-u)(1-u^2)}$$

Euler!formula

In general

$$(1-u)P_n = \sum_{i_n > i_{n-1} > \cdots i_1 \geq 0} u^{i_n + i_{n-1} + \cdots + i_1} - \sum_{i_n > i_{n-1} > \cdots i_1 \geq 0} u^{i_n + i_{n-1} + \cdots + (i_1+1)} \tag{R.20}$$

$$= u^{-1} \sum_{i_n > i_{n-1} > \cdots i_2 \geq 1} u^{i_n + i_{n-1} + \cdots + 2i_2} \tag{R.21}$$

since only the term $i_1 = i_2 - 1$ survives. Repeating this trick

$$(1-u)(1-u^2)P_n = u^{-1-2} \sum_{i_n > i_{n-1} > \cdots i_3 \geq 2} u^{i_n + i_{n-1} + \cdots + 3i_3}$$

and

$$\prod_{i=1}^{n} (1-u^i)\, P_n = u^{-(1+2+\cdots+n)} u^{n(n-1)} = u^{n(n-1)/2}$$

Thus

$$P_n = \frac{u^{n(n-1)/2}}{\prod_{i=1}^{n}(1-u^i)}.$$

(Adam Prügel-Bennet)

Solution 16.3: Euler formula, 2nd method. *The coefficients Q_k in (16.4) are given explicitly by the* Euler formula

$$Q_k = \frac{1}{1-\Lambda^{-1}} \frac{\Lambda^{-1}}{1-\Lambda^{-2}} \cdots \frac{\Lambda^{-k+1}}{1-\Lambda^{-k}} \quad . \tag{R.22}$$

Such a formula is easily proved by considering the finite order product

$$\mathcal{W}_j(z,\gamma) = \prod_{l=0}^{j} (1+z\gamma^l) = \sum_{l=0}^{j+1} \Gamma_l z^l$$

Since we have that

$$(1+z\gamma^{j+1})\mathcal{W}_j(z,\gamma) = (1+z)\mathcal{W}_j(\gamma z,\gamma)\,,$$

we get the following identity for the coefficients

$$\Gamma_m + \Gamma_{m-1}\gamma^{j+1} = \Gamma_m \gamma^m + \Gamma_{m-1}\gamma^{m-1} \quad m = 1, \ldots .$$

Starting with $\Gamma_0 = 1$, we recursively get

$$\Gamma_1 = \frac{1-\gamma^{j+1}}{1-\gamma} \qquad \Gamma_2 = \frac{(1-\gamma^{j+1})(\gamma-\gamma^{j+1})}{(1-\gamma)(1-\gamma^2)} \ldots .$$

the Euler formula (16.5) follows once we take the $j \to \infty$ limit for $|\gamma| < 1$.

(Robert Artuso)

Solution 16.3: Euler formula, 3rd method. *First define*

$$f(t,u) := \prod_{k=0}^{\infty}(1+tu^k) \; . \tag{R.23}$$

Note that

$$f(t,u) = (1+t)f(tu,u) \; , \tag{R.24}$$

by factoring out the first term in the product. Now make the ansatz

$$f(t,u) = \sum_{n=0}^{\infty} t^n g_n(u) \; , \tag{R.25}$$

plug it into (R.24), compare the coefficients of t^n and get

$$g_n(u) = u^n g_n(u) + u^{n-1} g_{n-1}(u) \; . \tag{R.26}$$

Of course $g_0(u) = 1$. Therefore by solving the recursion (R.26) and by noting that $\sum_{k=1}^{n-1} k = \frac{n(n-1)}{2}$ one finally arrives at

$$g_n(u) = \frac{u^{\frac{n(n-1)}{2}}}{\prod_{k=1}^{n}(1-u^k)} \; . \tag{R.27}$$

Euler got this formula and he and Jacobi got many nice number theoretical results from it, most prominent the pentagonal number theorem, which says that in the series expansion of $\prod_{k=1}^{\infty}(1-q^k)$ all terms cancel except those which have as an exponent the circumference of a regular pentagon with integer base length. recheck the tricks from PC's notebooks

(Juri Rolf)

Solution 16.4: 2-d product expansion. *Now let us try to apply the same trick as above to the two dimensional situation*

$$h(t,u) := \prod_{k=0}^{\infty}(1+tu^k)^{k+1} \; . \tag{R.28}$$

Write down the first terms and note that similar to (R.24)

$$h(t,u) = f(t,u)h(tu,u) \;, \tag{R.29}$$

where f is the Euler product (R.23). Now make the ansatz

$$h(t,u) = \sum_{n=0}^{\infty} t^n a_n(u) \tag{R.30}$$

and use the series expansion for f in (R.29) to get the recursion

$$a_n(u) = \frac{1}{1-u^n} \sum_{m=0}^{n-1} u^m a_m(u) g_{n-m}(u) \;. \tag{R.31}$$

With this one can at least compute the generalized Euler product effectively, but it would be nice if one could use it for a proof of the general behaviour of the coefficients a_n.

(Juri Rolf)

Chapter 17

Solution 17.4: Stability of billiard cycles. *The 2-cycle $\overline{0}$ stability (8.1) is the solution to both problems (provided you evaluate correctly the hyperbola curvature on the diagonal).*

Solution 17.5: Numerical cycle routines. *A number of sample Fortran programs for finding periodic orbits is available on the homepage for this manuscript,* `www.nbi.dk/ChaosBook/`.

Solution 17.12: Inverse iteration method for a Hamiltonian repeller. *For the complete repeller case (all binary sequences are realized), the cycles can be evaluated variationally, as follows. According to (3.12), the coordinates of a periodic orbit of length n_p satisfy the equation*

$$x_{p,i+1} + x_{p,i-1} = 1 - a x_{p,i}^2 \;, \quad i = 1, ..., n_p \;, \tag{R.32}$$

with the periodic boundary condition $x_{p,0} = x_{p,n_p}$.

In the complete repeller case, the Hénon map is a realization of the Smale horseshoe, and the symbolic dynamics has a very simple description in terms of the binary alphabet $\epsilon \in \{0,1\}$, $\epsilon_{p,i} = (1+S_{p,i})/2$, where $S_{p,i}$ are the signs of the corresponding cycle point coordinates, $S_{p,i} = x_{p,i}/|x_{p,i}|$. We start with a preassigned sign sequence $S_{p,1}, S_{p,2}, \ldots, S_{p,n_p}$, and a good initial guess for the coordinates $x'_{p,i}$. Using the inverse of the equation (17.22)

$$x''_{p,i} = S_{p,i} \sqrt{\frac{1 - x'_{p,i+1} - x'_{p,i-1}}{a}}, \quad i = 1, ..., n_p \tag{R.33}$$

we converge iteratively, at exponential rate, to the desired cycle points $x_{p,i}$. Given the cycle points, the cycle stabilities and periods are easily computed using (4.36). The itineraries and the stabilities of the short periodic orbits for the Hénon repeller (R.32) for $a = 6$ are listed in table 17.2; in actual calculations all prime cycles up to topological length $n = 20$ have been computed.

(G. Vattay)

⇓PRIVATE

center of mass
periodic!orbit condition
cycle!prime
prime cycle
prime cycle!count
Moebius inversion

Solution 17.13: "Center of mass" puzzle.** *(most of the text extracted from the ChaosBook.org boyscout, ChaosBook.org/version 11.5, Oct 29 2005 tex files)*

These extracts from ChaosBook.org are meant to complement and perhaps add to the Endler and Gallas [EG] explanation [R.2] of the "center of mass" puzzle for the cycles listed in table 17.2, first observed numerically by G. Vattay in ref. [R.1]. The main new material here is the observation that the time reversal invariance induces the factorizations of $S_n(\sigma)$ polynomials observed by EG. The symbolic dynamics notation for prime cycles and periodic points makes the time reversal symmetry explicit, and is therefore emphasized throughout.

Prime cycles and periodic points

A periodic point is a solution (x, n), $x \in \mathbb{R}^d$, $n \in \mathbb{Z}$ of the periodic orbit condition

$$x = f^n(x) \tag{R.34}$$

for a given mapping f. Each periodic point $x = x_{p,i} \in p$ belongs to a prime cycle p of period n_p, and its n_p distinct images $f^k(x_{p,i}) = x_{p,i+k}\,,\quad i+k$ mod n_p are the successive periodic points along the cycle.

A prime cycle *p of period n_p is a single traversal of the orbit. A prime cycle has a non-repeating symbol string: for example, $p = \overline{011} = \overline{101} = \overline{110} = \ldots 011011 \ldots$ is prime, but $\overline{0101} = 010101 \ldots = \overline{01}$ is not.*

extracted from count.tex, chapter 13

Let M_n be the number of prime *cycles of period n for a dynamical system whose symbolic dynamics is built from 2 symbols. There are 2^n possible distinct strings (periodic point labels) of length n composed of 2 letters. These 2^n periodic points include all M_d prime d-cycles whose period d equals or divides n.*

A prime d-cycle contributes d periodic points to the sum of all possible periodic points, one for each cyclic permutation. The total number of possible periodic symbol sequences of length n is therefore related to the number of prime cycles by

$$2^n = \sum_{d|n} dM_d\,.$$

The number of prime cycles can be computed recursively

$$M_n = \frac{1}{n}\left(2^n - \sum_{d|n}^{d<n} dM_d\right)\,,$$

or by the Möbius inversion formula

$$M_n = \frac{1}{n}\sum_{d|n}\mu\left(\frac{n}{d}\right)2^d\,. \tag{R.35}$$

where the Möbius function $\mu(1) = 1$, $\mu(n) = 0$ if n has a squared factor, and $\mu(p_1p_2\ldots p_k) = (-1)^k$ if all prime factors are different.

We list the number of prime cycles up to length 10 for the 2-letter complete symbolic dynamics in tables R.1 and R.2 (see table 13.2).

table R.1 derived from knead.tex, chapter 11

table R.1 derived from knead.tex, chapter 11

extracted from smale.tex, chapter 12

n_p	M_n	p	symmetry	S_s, S_b
1	2	0	x_0	$S_b = \sigma^2 + 2\sigma - a$
		1	x_1	
2	1	01		$S_s = \sigma - 2$
3	2	001	x_{010}	$S_b = \sigma^2 - 2\,\sigma + 2 - a$
		011	x_{101}	
4	3	0001		$S_s = \sigma^2 - 4\,a$
		0111		
		0011	x_{1001}, x_{0110}	$S_b = \sigma$
5	6	00001	x_{00100}	$S_b = \sigma^6 - 2\,\sigma^5 - 78\,\sigma^4 + 240\,\sigma^3$
		00011	x_{10001}	$+840\,\sigma^2 - 2496\,\sigma + 1448$
		00101	x_{01010}	(for $a = 6$)
		00111	x_{01110}	
		01011	x_{10101}	
		01111	x_{11011}	

Table R.1: Prime cycles for the binary symbolic dynamics up to length 5. They are all self-dual under time reversal, either with no point on the $x = y$ symmetry line, or points on it. "Symmetry" column contains - for self-dual cycles who have them - the cycle points on the $x = y$ diagonal. The number of prime cycles M_n is computed from (R.35), and S_s, S_b, polynomial factors (R.59), are taken from ref. [R.2].

n_p	M_n	p	symmetry
6	9	000001	
		000101	
		000111	
		010111	
		011111	
		001111	x_{011110}, x_{110011}
		000011	x_{001100}, x_{100001}
		001011	001101
7	18	0000001	$x_{0001000}$
		0000011	$x_{1000001}$
		0000101	$x_{0010100}$
		0001001	$x_{0100010}$
		0000111	$x_{0011100}$
		0010011	$x_{1001001}$
		0010101	$x_{0101010}$
		0001111	$x_{1100011}$
		0011011	$x_{0110110}$
		0101011	$x_{1010101}$
		0011111	$x_{0111110}$
		0101111	$x_{1101011}$
		0110111	$x_{1011101}$
		0111111	$x_{1110111}$
		0001011	0001101
		0010111	0011101

n_p	M_n	p	symmetry
8	30	00000001	
		00000101	
		00000111	
		00010101	
		00100101	
		00011011	
		00100111	
		00011111	
		01010111	
		01011011	
		01011111	
		01111111	
		00000011	$x_{00011000}$, $x_{10000001}$
		00001001	$x_{00100100}$, $x_{01000010}$
		00001111	$x_{00111100}$, $x_{11000011}$
		00101101	$x_{01011010}$, $x_{10100101}$
		00111111	$x_{11100111}$, $x_{01111110}$
		01101111	$x_{11011011}$, $x_{10111101}$
		00001011	00001101
		00010011	00011001
		00010111	00011101
		00110101	00101011
		00101111	00111101
		00110111	00111011
9	56		
10	99		

Table R.2: Prime cycles for the binary symbolic dynamics lengths 6 to 10. Starting with cycle length 6, a cycle is either self-dual under time reversal, or has a time-reversed partner. A self-dual cycle either has no point on the $x = y$ symmetry line, or has points on it. "Symmetry" column contains the other prime cycle belonging to a time-reversal pair, or - for self-dual cycles who have them - the cycle points on the $x = y$ diagonal.

Moebius inversion

Consider the n-periodic point condition $0 = f^n(x) - x$. This polynomial of order 2^n has zeros at all shorter, period d prime cycles if d is a divisor of n. Dividing those out, we arrive at the polynomial [R.6]

$$Q_n(x) = \prod_{d|n} \left(f^d(x) - x\right)^{\mu(n/d)} , \tag{R.36}$$

with nM_n zeros corresponding to the n periodic points for each prime cycle p of period $n_p = n$, $Q_n(x) = \prod_p P_p(x)$, where the nth order polynomial

$$P_p(x) = \prod_{i \in p}(x - x_{p,i}) = 0 , \qquad n_p = n \tag{R.37}$$

has zeros at all periodic points in prime cycle p. Except for some values of a, at which bifurcations occur, these are simple zeros.

The coefficients in the expansion of (R.41) are symmetric polynomials in x_i, all reducible to powers of

$$\sigma_p = \sum_{i \in p} x_{p,i} \tag{R.38}$$

and a. For example, the x^{n-2} coefficient

$$2 \sum_{i<j} x_i x_j = \sigma^2 - \sum_i x_i^2 = \sigma^2 + 2\sigma - n_p a$$

can be expressed in terms of σ^2, σ and a

$$P_p(x) = x^{n_p} - \sigma_p x^{n_p - 1} + (\sigma^2 + 2\sigma - n_p a) x^{n_p - 2} + \cdots \pm (\sigma^{n_p} \cdots) . \tag{R.39}$$

We refer to σ as the "center of mass" of cycle p (up to an overal prefactor of $1/n_p$).

By cyclic invariance of periodic points in p, σ_p is invariant under $x \to f(x)$, so it is an intrinsic property of the prime cycle p, hence it can take at most M_n distinct values corresponding to the M_n prime cycles p of period $n_p = n$.

EG succeeded - after considerable algebra - in computing explicitely the M_n-th order polynomials

$$S_n(\sigma) = 0 , \tag{R.40}$$

fill in the explanation

for $n_p \le n$. The M_n root $\sigma = \sigma_p$ substituted into the nth order polynomial

$$P_n(x, \sigma_p, a) = \prod_{i \in p}(x - x_i) = 0 , \tag{R.41}$$

Henon@Hénon!map!stability

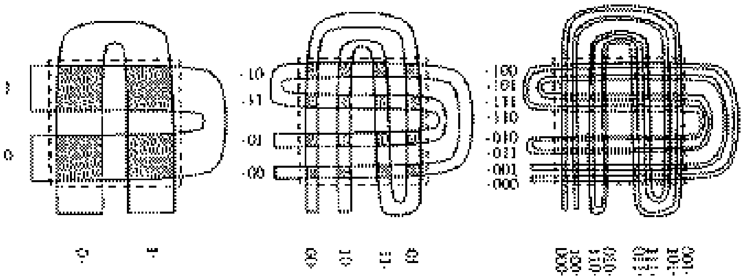

Figure R.3: A complete Smale horseshoe iterated forwards and backwards, orientation preserving case: function f maps the dashed border square $\mathcal{M}$ into the vertical horseshoe, while the inverse map f^{-1} maps it into the horizontal horseshoe. a) One iteration, b) two iterations, c) three iterations. The non–wandering set is contained within the intersection of the forward and backward iterates (crosshatched). (from K.T. Hansen [1.3])
DRAW THE RIGHT ONE, with 1-fixed point at the top right corner.

yields the n periodic points $x = x_{p,i}$ belonging to the prime cycle p as the roots of $P_n(x, \sigma_p, a) = 0$. As the reduction of symmetric polynomial coefficients does not rely on the shape of a given prime cycle p, P_n has the same form for all $n_p = n$.

Smale horseshoe

Smale horseshoes and symbolic dynamics labeling of the dynamics - it's really great, once you get it, because the label tells you everything about the cycle point and the cycle it belongs too. From table R.1 you can read off the shape and symmetry of individual cycles, and the factorization of S - at least the highest power of σ in each of the monic polynomials it factors into.

The Hénon map is kind of a fattened parabola. It takes a rectangular initial area and returns it bent as a horseshoe, such that the initial area is intersected twice, see Figure R.3.

Figure R.3 from exercise 12.4

The map (??) is quadratic, with two fixed points:

from exercise 3.4

$$x_0 = -1 - \sqrt{1+a}\,, \qquad x_1 = -1 + \sqrt{1+a}\,, \tag{R.42}$$

indicated in figure R.4 (a). The $\overline{01}$ periodic points are

from example 4.7

$$x_{10} = 1 + \sqrt{a-3}\,, \qquad x_{01} = 1 - \sqrt{a-3}\,. \tag{R.43}$$

The Jacobian matrix for the nth iterate of the Hamiltonian Hénon map is

$$\mathbf{J}^n(x_0) = \prod_{m=n}^{1} \begin{pmatrix} -2x_m & -1 \\ 1 & 0 \end{pmatrix}, \qquad x_m = f_1^m(x_0, y_0)\,. \tag{R.44}$$

main text - explain the order of multiplication

The determinant of the Hénon one time-step Jacobian matrix (R.44) is constant,

$$\det \mathbf{J} = \Lambda_1 \Lambda_2 = 1 \tag{R.45}$$

Henon@Hénon!map!fixed points
stable!manifold
unstable!manifold

so only one eigenvalue $\Lambda_1 = 1/\Lambda_2$ needs to be determined. Both fixed points are hyperbolic for $a > 3$, with expanding eigenvalues

$$
\begin{aligned}
\Lambda_0 &= 1 + (1+a)^{1/2} + (1+a)^{1/4}((1+a)^{1/2}+2)^{1/2} \\
\Lambda_1 &= 1 - (1+a)^{1/2} - (1+a)^{1/4}((1+a)^{1/2}-2)^{1/2} ,
\end{aligned}
\tag{R.46}
$$

see sect. 12.1

As $\Lambda_0 > 0$, x_0 fixed point sits at the edge of the non–wandering set. For $a = 6$ this is a strongly unstable fixed point, with $\Lambda_0 = 7.15\ldots$. If we track to the right W_0^s, the stable manifold of the x_0 fixed point, and upwards W_1^u, the unstable manifold of x_0 fixed point, their intersection encloses the crosshatched region $\mathcal{M}_.$. Any point outside W_0^u border of $\mathcal{M}_.$ escapes to infinity forward in time, while any point outside W_0^s border escapes to infinity backwards in time. In this way the unstable–stable manifolds define topologically invariant and optimal $\mathcal{M}_.$ initial region; all orbits that stay confined for all times are confined to $\mathcal{M}_.$. An orbit with a subsequence of m consecutive 0 moves approximately along a hyperbola which has to get as close as $1/\Lambda_0^m$ to x_0 in order to stay for m iterations on the left side.

move to symbolic dynamics section

The other fixed point x_1 unstable eigenvalue is not as large, $\Lambda_1 = -2.95\ldots$, It is negative, implying that the neighborhood of x_1 turns by 180^o in each iteration.

Taken together, these two observations almost produce the symbolic dynamics rules for determining diagonal crossings, but not quite. Between

$$01\cdots \to 10\cdots \textit{ and } 10\cdots \to 01\cdots$$

there is always a diagonal crossing. Two fixed points 0 and 1 are special. Beyond that, every string of 0^m crosses once, and most $1\cdots \to \cdots$ imply a diagonal crossing, but precise rule is missing still.

A plot in the symbol plane (where unstability is roughly factor 2 by construction) would not have the points closest to x_0, x_1 look so much like they lie on the symmetry diagonal.

create figure R.4 for $b = -1$

Using instead the conjugacy by reversor seems hard, as in that case one needs to flip the global label of symbolic sequence between to crossing diagonal one way, and then returning again. Maybe it is not such a big deal, as long strings that stay on on side have to do with long 0^m blocks of symbols.

Iterated one step forward, the region $\mathcal{M}_.$ is stretched and folded into a Smale horseshoe *drawn in figure R.4 (b). The horseshoe "fattened parabola" shape is the consequence of the quadratic form x^2 in (??). Label the two forward intersections $f(\mathcal{M}_.) \cap \mathcal{M}_.$ by $\mathcal{M}_{s.}$, with $s \in \{0,1\}$, figure R.4 (b). The horseshoe consists of the two strips $\mathcal{M}_{0.}, \mathcal{M}_{1.}$, and the bent segment that lies entirely outside the W_1^u line. As all points in this segment escape to infinity under forward iteration, this region can safely be cut out and thrown away.*

Iterated one step backwards, the region $\mathcal{M}_.$ is again stretched and folded into a horseshoe, figure R.4 (c). As stability and instability are interchanged under time reversal, this horseshoe is transverse to the forward one. Again the points in the horseshoe bend wonder off to infinity as $n \to -\infty$, and we are left with the two (backward) strips $\mathcal{M}_{.0}, \mathcal{M}_{.1}$. Iterating two steps forward we obtain the four strips $\mathcal{M}_{11.}, \mathcal{M}_{01.}, \mathcal{M}_{00.}, \mathcal{M}_{10.}$, and iterating backwards we obtain the four strips $\mathcal{M}_{.00}, \mathcal{M}_{.01}, \mathcal{M}_{.11}, \mathcal{M}_{.10}$ transverse to the forward ones. Iterating three steps forward we get an 8 strips, and so on ad infinitum.

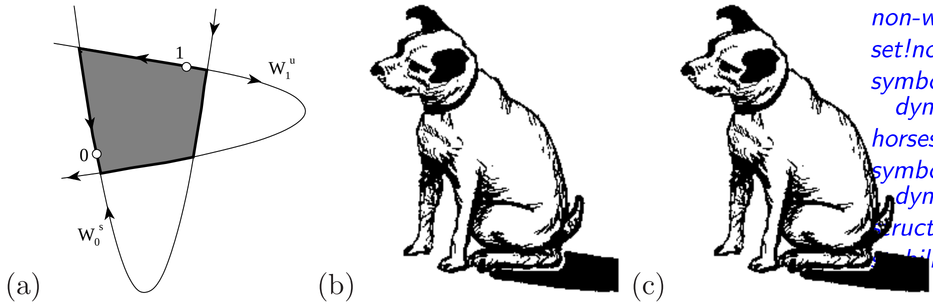

non-wandering set
set!non-wandering
symbolic dynamics!complete
horseshoe!complete
symbolic dynamics!unimodal
structural stability
stability!structural

Figure R.4: The Hénon map for $a = 6$, $b = -1$. (a) The fixed points $\overline{0}$, $\overline{1}$, and the segments of the W_1^s stable manifold, W_1^u unstable manifold that enclose the initial (crosshatched) region $\mathcal{M}_.$. (b) The forward horseshoe $f(\mathcal{M}_.)$. (c) The backward horseshoe $f^{-1}(\mathcal{M}_.)$. Iteration yields a complete Smale horseshoe, with every forward fold intersecting every backward fold.
DRAW THE RIGHT ONE, with 1-fixed point at the top right corner.

Symbolic dynamics

The two strips $\mathcal{M}_{.0}, \mathcal{M}_{.1}$ partition the phase space into two regions labeled by the two-letter alphabet $\mathcal{A} = \{0, 1\}$. $S^+ = .011$ is the future itinerary *for all $x \in \mathcal{M}_{.011}$. Likewise, for the forward strips all $x \in \mathcal{M}_{s_{-m}\cdots s_{-1}s_0.}$ have the* past itinerary *$S^- = s_{-m}\cdots s_{-1}s_0$. Ω, the non–wandering set (2.2) of $\mathcal{M}_.$, is the union of all points whose forward and backward trajectories remain trapped for all time, is given by the intersections of all images and preimages of $\mathcal{M}$:*

$$\Omega = \left\{ x : x \in \lim_{m,n\to\infty} f^m(\mathcal{M}) \bigcap f^{-n}(\mathcal{M}) \right\} . \tag{R.47}$$

For a complete *Smale horseshoe every forward fold $f^n(\mathcal{M})$ intersects transversally every backward fold $f^{-m}(\mathcal{M})$, so a unique bi-infinite binary sequence can be associated to every element of the non–wandering set. A point $x \in \Omega$ is labeled by the intersection of its past and future itineraries $S(x) = \cdots s_{-2}s_{-1}s_0.s_1s_2\cdots$, where $s_n = s \quad \text{if} \quad f^n(x) \in \mathcal{M}_{.s}$, $s \in \{0, 1\}$ and $n \in \mathbb{Z}$.*

As a increases, the dynamics become increasingly chaotic, and beyond a critical value, $a = a_H$, the set of bounded orbits forms a Smale horseshoe (this set has measure zero—almost all orbits escape to infinity). It was proved by Devaney and Nitecki that there is indeed a hyperbolic horseshoe when $a > 5 + 2\sqrt{5} > a_H$ [R.12, 34.8]. Our numerical studies indicate that [34.8, ?]

$$a_H \approx 5.699310786700 . \tag{R.48}$$

extracted from knead.tex, chapter 11

Example: *The trajectory $x_1, x_2, x_3, \ldots$ of the initial point x_0 is given by the iteration $x_{n+1} = f(x_n)$. Iterating f and checking the sign of x_k associates a* temporally ordered *topological itinerary $s_{-m}\cdots s_{-1}s_0$ with a given trajectory,*

$$s_k = \begin{cases} 1 & \text{if } x_k > 0 \\ 0 & \text{if } x_k < 0 \end{cases} . \tag{R.49}$$

The system is said to be structurally stable *if all intersections of forward and backward iterates of $\mathcal{M}$ remain transverse for sufficiently small perturbations $f \to f + \delta$ of the flow.*

For the Hamiltonian Hénon map the numerical work indicates that for

$$a > 5.699310786700\,. \tag{R.50}$$

the map has a complete Smale horseshoe. For example, for sufficiently small variations of a the Hénon map studied here numerically for $a = 6$ is structurally stable.

Example: *How do we know that the cycles in figure R.7 are $\overline{0001011}$, $\overline{0001101}$? Easy, for the $a = 6$ case the symbolic dynamics is obtained by (R.49), by simply noting the sign of x_n. If you actually plot first few iterates of the forward and backward horseshoe in figure R.4, you will see that your periodic points sit in the strips labeled as above.*

Time reversal symmetry

from appendix J - Discrete symmetries, appendix J.5

Under the time reversal

$$\cdots s_{-2}s_{-1}s_0.s_1s_2s_3\cdots \to \cdots s_3s_2s_1.s_0s_{-1}s_{-2}\cdots$$

the points in the symbol square for an orientation preserving map are symmetric across the diagonal $\gamma = \delta$. Consequently the periodic orbits appear either in dual pairs $p = s_1s_2s_3\ldots s_n$, $\overline{p} = s_ns_{n-1}s_{n-2}\ldots s_1$, or are self-dual under time reversal, $S_p = S_{\overline{p}}$.

insert this into the book

For the orientation preserving case a self-dual cycle of odd period has at least one point (or odd number of points) on the symmetry diagonal. In particular, all fixed points lie on the symmetry diagonal. A self-dual cycle of even period has no, or even number of points on the symmetry diagonal.

from symm.tex, chapter 22 - Discrete symmetries, sect. 22.1.2

Consider f, a map on the interval with reflection symmetry $f(-x) = -f(x)$. A simple example is the piecewise-linear sawtooth map of figure R.5. Denote the reflection operation by $\mathbf{C}x = -x$. The symmetry of the map implies that if $\{x_n\}$ is a trajectory, than also $\{\mathbf{C}x_n\}$ is a trajectory because $\mathbf{C}x_{n+1} = \mathbf{C}f(x_n) = f(\mathbf{C}x_n)$. The dynamics can be restricted to a fundamental domain, in this case to one half of the original phase space; every time a trajectory leaves this domain, it can be mapped back using $\mathbf{C}$. $\mathbf{C}$ satisfies $\mathbf{C}^2 = \mathbf{e}$ and can be used to decompose the phase space into mutually orthogonal symmetric and antisymmetric subspaces by means of projection operators (22.1).

try to define $\mathcal{L}$ whose eigenvalues are σ_p, or $x_{p,1}$

One distinguishes three kinds of cycles: asymmetric cycles a, symmetric cycles s built by repeats of irreducible segments $\tilde{s}$, and boundary cycles b.

Asymmetric cycles: *A periodic orbits is not symmetric if $\{x_a\} \cap \{\mathbf{R}x_a\} = \emptyset$, where $\{x_a\}$ is the set of periodic points belonging to the cycle a. Thus $\mathbf{R}$ generates a second orbit with the same number of points and the same stability properties.*

For this class of cycles for any n,

$$P_a(x, \sigma, a) = \prod^{p} (x - x_{a,i}) \tag{R.51}$$

has n distinct roots $\{x_{a,i}\}$. The associated equation for is $A(\sigma)^2 = 0$.

Example: *Follow the succeessive cycle points in the prime cycle $\overline{0001011}$, figure R.7(a); then flip across the diagonal, reverse the direction along the cycle, and you are now on the the prime cycle $\overline{0001101}$, the time reversed partner of $\overline{0001011}$.*

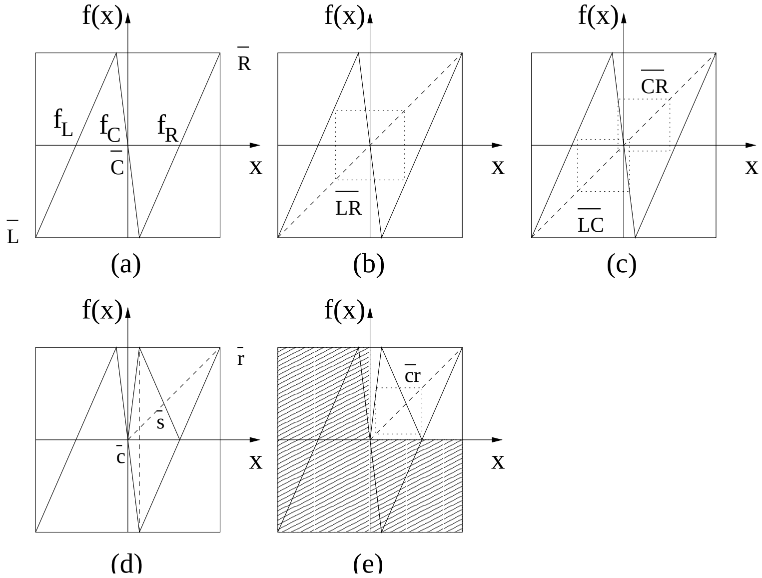

Figure R.5: The Ulam sawtooth map with the C_2 symmetry $f(-x) = -f(x)$. (a) boundary fixed point $\overline{C}$, (b) symmetric 2-cycle $\overline{LR}$, (c) asymmetric 2-cycles pair $\{\overline{LC},\overline{CR}\}$. The Ulam sawtooth map restricted to the fundamental domain; pieces of the global map (a) are reflected into the upper right quadrant. (d) Boundary fixed point $\overline{C}$ maps into the fixed point $\overline{c}$, symmetric 2-cycle $\overline{LR}$ maps into fixed point $\overline{s}$, and the asymmetric fixed point pair $\{\overline{L},\overline{R}\}$ maps into a single fixed point $\overline{r}$, (e) the asymmetric 2-cycles pair $\{\overline{LC},\overline{CR}\}$ maps into a single 2-cycle $\overline{cr}$.

Symmetric cycles, no boundary point: *A cycle s is reflection symmetric if operating with $\mathbf{R}$ on the set of cycle points reproduces the set. The period of a symmetric cycle is always even ($n_s = 2m$) and the mirror image of the x_s cycle point is reached by traversing the irreducible segment $\tilde{s}$ of length m, $f^m(x_s) = \mathbf{R}x_s$.*

$$P_C(x,\sigma,a) = (x-x_1)(x-x_2)^2 \cdots (x-x_m)^2(x-x_{m+1}) \tag{R.52}$$

has $m+1$ distinct roots.

$$\sigma_p = x_1 + 2x_2 + \cdot + 2x_m + x_{m+1} \tag{R.53}$$

Example: *Symmetric (or self-dual orbit):*
Draw 4-cycles $\overline{0001}$ and $\overline{0111}$. They map into themselves under flip and time reversal. That means that if you know 2 cycle points, the other 2 are given by symmetry.

Even symmetric cycles, 2 boundary points:

$$P_s(x,\sigma,a) = \prod^{p}(x-x_{s,i})^2 \tag{R.54}$$

has $n_{\tilde{s}}$ distinct roots.

$$\sigma_p = 2\sum_i^{n_{\tilde{s}}} x_{p,i} \tag{R.55}$$

3 or more boundary points are not possible for prime cycles.

Cycle $\overline{0011}$ is an example of even-period boundary prime cycle . Two periodic points x_{1001}, x_{0110} are on the symmetry diagonal, and reflection symmetry of the remaining x_{0011}, x_{1100} pair forces a square-shaped trajectory in the $[x, y]$ plane, see figure R.6:

make into an exercise

$$\left[\begin{pmatrix} x_{1001} \\ x_{1001} \end{pmatrix}, \begin{pmatrix} -x_{1001} \\ x_{1001} \end{pmatrix}, \begin{pmatrix} -x_{1001} \\ -x_{1001} \end{pmatrix}, \begin{pmatrix} x_{1001} \\ -x_{1001} \end{pmatrix}\right]$$

Hence $\sigma_{0011} = 0$, and

$$P_{0011} = (x^2 - x_{0011}^2)^2 \,. \tag{R.56}$$

with $x_{0011} = \sqrt{a}$. Note that this 4-cycle is more robust than the 2-cycle given in (R.43) - it exists for $a > 0$, and is not the period-doubling relative of the 2-cycle.

Odd symmetric cycles $n = 2m + 1$, 1 boundary point:

$$P_B(x, \sigma, a) = (x - x_1)^2 \cdots (x - x_m)^2 (x - x_{m+1}) \tag{R.57}$$

has $m + 1$ distinct roots.

$$\sigma_p = 2x_1 + 2x_2 + \cdot + 2x_m + x_{m+1} \tag{R.58}$$

Example: *Boundary cycles:*
Draw 3-cycles $\overline{001}$ and $\overline{011}$. They have a point on the diagonal, indicated in the table S.1.

The time reversal symmetry of the phase space (this is true for all *Hamiltonian time-reversible flows whose Poincare section is symmetric under $[q, p] \to [p, q]$ diagonal flip, not just polynomial mappings) implies - but we need to cleanly explain it for this case (ChaosBook.org proves it for discrete space symmetry groups) that $S_n(\sigma)$* always *factorizes into form*

$$S = A^2 BC. \tag{R.59}$$

EG indeed observe that the polynomials $S = S_n(\sigma)$ factorize into product of polynomials over the above three kinds of cycles.

To verify, compare $S_1, S_2, \cdots, S_8$ of ref. [R.2] with the listing of 3 kinds of cycles in table R.1; the number of cycles of each type determines the order of the corresponding S_n polynomial. The order of A is the number of time-reversed pairs in table R.1. The order of B is the number of symmetric cycles in table R.1, and the order of C is the number of boundary cycles in table R.1.

For each n, the $P_n(x, \sigma, a)$ polynomial should be written explicitely for each of the 3 symmetry classes $[a, s, b]$. In particular, for $P_s(x, \sigma, a)$ the factorization over 1/2 of the phase space

$$P_s(x, \sigma, a) = \left(\prod^{\tilde{s}} (x - x_{\tilde{s},i})\right)^2 \tag{R.60}$$

is expected, as exemplified by the 6-cycle figure R.6(c).

center of mass

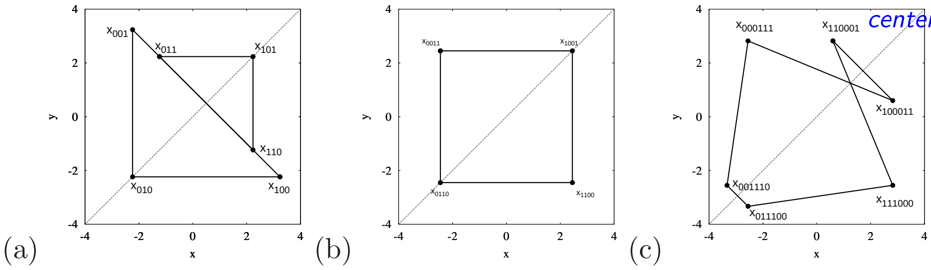

Figure R.6: The Hénon map for $a = 6$, $b = -1$. (a) The boundary 3-cycles $\overline{001}$, $\overline{011}$. Any odd period cycle has odd number of points on the boundary. (b) The boundary 4-cycle $\overline{0011}$. (c) A symmetric 6-cycle $\overline{000111}$.

Remark R.1 "Center of mass" puzzle. The "center of mass" notions play important role in a number of physical problems, such as: (1) the periodic-orbit formulation of the deterministic drift and diffusion (chapter 23), (2) the kinematic dynamo problem [R.1, R.33] (appendix I), and (3) Sullivan's formulation [R.34, R.35, R.36, R.37] of the Feigenbaum δ eigenvalue problem in the period-doubling renormalization theory.

The "center of mass" puzzle for the cycles listed in table 17.2 was first observed numerically by G. Vattay in ref. [R.1], and was resolved by Endler and Gallas [R.2].

EG method of solution resembles the methods earlier employed for quadratic polynomials (and thier Julia sets) by Brown [R.27] and Stephenson [R.29]. Brown gives cycles up to length 6 for the logistic map, employing symmetric functions of cycle points. Hitzl and Zele [R.31] study the of the Hénon map for cycle lengths up to period 6.

All explicit values of periodic points for the Hamiltonian Hénon mapping displayed here are taken from ref. [R.2]. Method of ref. [R.2] applies to cycles of polynomial maps only, in this case the quadratic map.

Remark R.2 Complete Smale horseshoe, Hamiltonian Hénon. Devaney and Nitecki [R.12] proved that the Hamiltonian Hénon map has a complete Smale horseshoe for $a > 5 + 2\sqrt{5}$. The numerical studies of refs. [?, R.17] indicates this holds for $a > 5.699310786700$.

Remark R.3 Symmetries of the symbol square. For a more detailed discussion of symmetry lines and the symbolic dynamics symmetries, see refs. [R.52, R.49, R.53]. It is an open question (see remark 22.4) as to how time reversal symmetry can be exploited for further reductions of cycle expansions. For example, the fundamental domain symbolic dynamics for reflection symmetric systems is discussed in some detail in sect. 22.5, but how does one recode from time-reversal symmetric symbol sequences to asymmetrized 1/2 phase space symbols? improve references

Remark R.4 Symbolic dynamics. Perhaps you should read K.T. Hansen's PhD thesis `ChaosBook.org/projects/KTHansen/thesis`. It explains all this in more detail and better than `ChaosBook.org`.

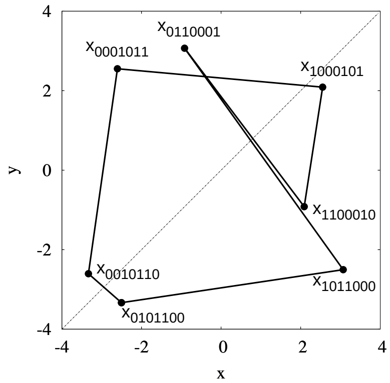

(a)

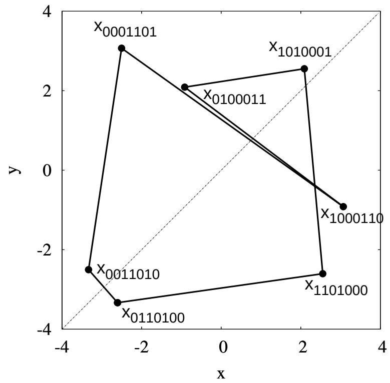

(b)

Figure R.7: The Hénon map for $a = 6$, $b = -1$, asymmetric cycles: (a) The 7-cycle $\overline{0001011}$, and (b) its partner $\overline{0001101}$ under flip across the diagonal and time-reversal. Note that under time reversal periodic points symbol sequences map into their symmetry partners point by point.

References

[R.1] *N.J. Balmforth, P. Cvitanović, G.R. Ierley, E.A. Spiegel and G. Vattay, "Advection of vector fields by chaotic flows,"* Stochastic Processes in Astrophysics, Annals of New York Academy of Sciences **706**, *148 (1993);* `preprint`.

[R.2] *A. Endler and J.A.C. Gallas, "Rational reductions of sums of orbital coordinates for a Hamiltonian repeller," draft (2005).*

[R.3] *A. Endler and J.A.C. Gallas, "Chiral orbits," draft (2005).*

[R.4] *P. Fatou,* Bull. Soc. Math. France **47**, *161 (1919); ibid.* **48**, *33 and 208 (1920).*

[R.5] *G. Julia,* J. Math. Pures et Appl. **4**, *47 (1918).*

[R.6] *J.W. Milnor, "Orbits, Externals Rays and the Mandelbrot Set: An Expository Account,"* `math.DS/99051690`.

[R.7] *W. Jung, "Some Explicit Formulas for the Iteration of Rational Functions," unpublished (1997);*
`ftp://work1.iram.rwth-aachen.de/pub/papers/jung/expl.pdf`.

[R.8] *R.L. Devaney,* An Introduction to Chaotic Dynamical Systems *(Addison-Wesley, Reading MA, 1987).*

[R.9] *J. Hale and H. Koçak,* Dynamics and Bifurcations *(Springer-Verlag, New York 1991).*

[R.10] *B.-L. Hao and W.-M. Zheng,* Applied Symbolic Dynamics and Chaos *(World Scientific, River Edge, NJ, 1998).*

[R.11] *M. Hénon, "Numerical study of quadratic area-preserving mappings,"* Quart. Appl. Math. **27**, *291 (1969).*

[R.12] *R.L. Devaney and Z. Nitecki, "Shift automorphisms in the Hénon mapping,"* Commun. Math. Phys. **67**, *137 (1979).*

[R.13] *J. Franks, "Periodic points and rotation numbers for area-preserving diffeomorphisms of the plane,"* Publ. Mathématiques de l'IHÉS **71**, *105 (1990).*

[R.14] *J.K. Moser, "On quadratic symplectic mappings,"* Math. Zeitschrift **216**, *417 (1994).*

[R.15] *H.P. Fang. "Dynamics for a two-dimensional antisymmetric map,"* J. Phys. A **27**, *5187 (1994).*

[R.16] Y. Aizawa. "Symbolic dynamics approach to the two-D chaos in area-preserving maps," Prog. Theor. Phys. **71**, 1419 (1984).

[R.17] D.G. Sterling, H.R. Dullin and J.D. Meiss, "Homoclinic Bifurcations for the Hénon Map," Physica D **134**, 153 (1999); `chao-dyn/9904019`.

[R.18] D.G. Sterling and J.D. Meiss, "Computing periodic orbits using the anti-integrable limit," Phys. Lett. A **241**, 46 (1999).

[R.19] H.R. Dullin, J.D. Meiss and D.G. Sterling, "Symbolic Codes for Rotational Orbits," `nlin.CD/0408015`.

[R.20] A. Gómez and J.D. Meiss, "Reversible Polynomial Automorphisms of the Plane: the Involutory Case," Phys. Lett. A **312**, 49 (2003); `nlin.CD/0209055`.

[R.21] A. Gómez and J.D. Meiss, " Reversors and symmetries for polynomial automorphisms of the complex plane," Nonlinearity **17**, 975 (2004).

[R.22] M. Baake and J.A.G. Roberts "Symmetries and reversing symmetries of polynomial automorphisms of the plane," `math.DS/0501151`.

[R.23] H.W.E. Jung, "Über ganze birationale Transformationen der Ebene," J. Reine Angew. Math. **184**, 161 (1942).

[R.24] J.S.W. Lamb and J.A.G. Roberts, "Time-reversal symmetry in dynamical systems: a survey," Physica D **112**, 1 (1998);
`www.ma.ic.ac.uk/~jswlamb/papers/survey.ps`

[R.25] C.R. Jordan, D.A. Jordan, and J.H. Jordan, "Reversible complex Henon maps," Experiment. Math. **11**, 339 (2002);
`www.expmath.org/expmath/volumes/11/11.3/Jordan339_347.pdf`.

[R.26] D.A. Jordan, "Iterations of the complex Henon map," Java applet,
`www.shef.ac.uk/~daj/henon/chm.html`.

[R.27] A. Brown, "Equations for periodic solutions of a logistic difference equation," J. Austral. Math. Soc (Series B) **23**, 78 (1981).

[R.28] J. Stephenson, "Formulae for cycles in the Mandelbrot set," Physica **A 177**, 416-420 (1991).

[R.29] J. Stephenson and D.T. Ridgway, "Formulae for cycles in the Mandelbrot set II," Physica **A 190**, 104-116 (1992).

[R.30] J. Stephenson, "Formulae for cycles in the Mandelbrot set III," Physica **A 190**, 117-129 (1992)

[R.31] D.L. Hitzl and F. Zele, Physica **D 14**, 305 (1985).

[R.32] K. Karamanos and I. Kotsireas "On the arithmetic nature of various constants at the accumulation points of unimodal maps and in particular of the logistic map," e-print (2003).

[R.33] S. Childress and A.D. Gilbert Stretch, Twist, Fold: The Fast Dynamo, Lecture Notes in Physics **37** (Springer Verlag, Berlin 1995).

[R.34] R. Artuso, E. Aurell and P. Cvitanović, "Recycling of strange sets II: Applications," Nonlinearity **3**, 361 (1990).

[R.35] F. Christiansen, P. Cvitanović and H.H. Rugh, "The spectrum of the period-doubling operator in terms of cycles," J. Phys **A 23**, L713 (1990).

[R.36] M. Pollicott, "A Note on the Artuso-Aurell-Cvitanović approach to the Feigenbaum tangnt operator," J. Stat. Phys., **62**, 257 (1991).

[R.37] Y. Jiang, T. Morita and D. Sullivan, "Expanding direction of the period doubling operator," Comm. Math. Phys. **144**, 509 (1992).

[R.38] *For a definition of resultant of two polynomials, see* `mathworld.wolfram.com/Resultant.html`.

[R.39] *I. Procaccia and R. Zeitak*, Phys. Rev. Lett. **60**, *2511 (1988).*

[R.40] *A.É. Eremenko and G.M. Levin, 'Periodic points of polynomials'*, Ukrain. Mat. J. **41**, *1258 (1989), [english translation].*

[R.41] *G. Levin, M. Sodin and P. Yuditskii, 'A Ruelle operator for a real Julia set'*, Comm. Math. Phys. **141**, *119 (1991).*

[R.42] *G. Levin, M. Sodin, and P. Yuditskii, 'Ruelle operators with rational weights for Julia sets'*, J. d'Analyse Math. 63, *303 (1994).*

[R.43] *A. Eremenko, G. Levin, and M. Sodin, 'On the distribution of zeros of a Ruelle zeta-function'*, Comm. Math. Phys. **159**, *433 (1994).*

[R.44] *G. Levin, 'On Mayer's conjecture and zeros of entire functions'*, Ergod. The. and Dynam Sys. **14**, *565 (1994).*

[R.45] *S. Hatjispiros and F. Vivaldi, "A family of rational zeta functions for the quadratic map,"* Nonlinearity **8**, *321 (1995).*

[R.46] *T. Bohr, P. Cvitanović and M.H. Jensen*, Europhys. Letts. **6**, *445 (1988).*

[R.47] *H.-O. Peitgen, H. Jürgens and D. Saupe*, Chaos and Fractals *(Springer-Verlag, Berlin 1992).*

[R.48] *P. Cvitanović and J. Myrheim*, Phys. Lett. **A94**, *329 (1983);* Commun. Math. Phys. **121**, 225 (1989)

[R.49] *C. Mira*, Chaotic Dynamics - From one dimensional endomorphism to two dimensional diffeomorphism, *(World Scientific, Singapore, 1987).*

[R.50] *G. D. Birkoff*, Rend. Circ. Mat. Palermo **39**, *265 (1915).*

[R.51] *R. De Vogélaere, in S. Lefschetz, ed.*, Contribution to the Theory of Nonlinear Oscillations *pp. 54–84 (Princeton Univ. Press, Princeton 1958)*

[R.52] *J.M. Greene*, J. Math. Phys. **20**, 1183 (1979)

[R.53] *P.H. Richter, H-J. Scholz and A. Wittek, "A Breathing Chaos,"* Nonlinearity **3**, *45 (1990).*

[R.54] *G.D. Birkhoff*, Dynamical systems, `Amer. Math. Soc. Colloq. Publ.` **9**, *(Amer. Math. Soc., Providence, RI 1955).*

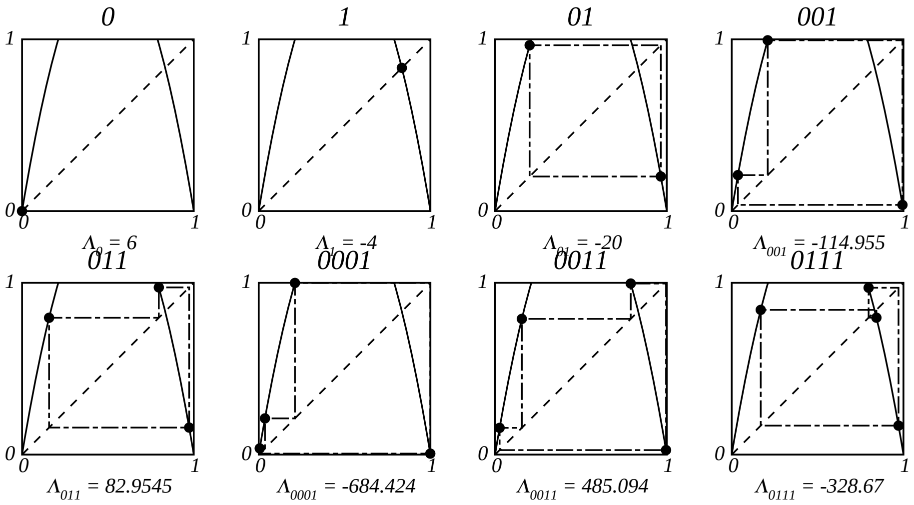

Figure R.8: Periodic orbits and stabilities for the logistics equation $x_{n+1} = 6x_n(1 - x_n)$.

⇑PRIVATE

Chapter 18

Solution 18.2: Prime cycles for a 1-d repeller, analytic formulas. *For the logistic map the prime cycles, ordered in terms of their symbolic dynamics, are listed in table 11.1*

$$\mathcal{P} = \{0, 1, 01, 001, 011, 0001, 0011, 0111, \ldots\}$$

The position of the prime cycles can be found by iterating the inverse mapping. If we wish to find the position of a prime orbit $p = b_1 b_2 \cdots b_{n_p}$, where $b_i \in \{0, 1\}$, then starting from some initial point, $x = 1/2$ say, we apply one of the inverse mappings

$$f_{\pm}^{-1}(x) = \frac{1}{2} \pm \frac{1}{2}\sqrt{1 - x/4A}$$

where we choose f_-^{-1} if $b_1 = 0$ or f_+^{-1} if $b_1 = 1$. We then apply the inverse mapping again depending on the next element in the prime orbit. Repeating this procedure many times we converge onto the prime cycle. The stability Λ_p of a prime cycle p is given by the product of slopes of f around the cycle. The first eight prime cycles are shown in figure R.8.

The stabilities of the first five prime orbits can be calculated for arbitrary A. We find that $\Lambda_0 = A$, $\Lambda_1 = 2 - A$, $\Lambda_{01} = 4 + 2A - A^2$, and

$$\Lambda_{\substack{001\\011}} = 8 + 2A - A^2 \pm A(2 - A)\sqrt{A^2 - 2A - 7}. \tag{R.61}$$

There is probably a closed form expression for the 4-cycles as well.

For crosschecking purposes: if $A = 9/2$, $\Lambda_0 = 9/2$ $\Lambda_1 = -5/2$ $\Lambda_{01} = -7.25$ $\Lambda_{011} = 19.942461\ldots$.

(Adam Prügel-Bennet)

Solution 18.2: Dynamical zeta function for a 1-d repeller *The escape rate can be estimated from the leading zero in the dynamical zeta function* $1/\zeta(z)$, *defined by*

$$1/\zeta(z) = \prod_p \left(1 - z^{n_p}/|\Lambda_p|\right) .$$

To compute the position of this pole we expand $1/\zeta(z)$ *as a power series (18.5) in* z

$$1/\zeta(z) = 1 - \sum_{i=1} \hat{c}_i z^i$$

where

$$\begin{aligned}
\hat{c}_1 &= |\Lambda_0|^{-1} + |\Lambda_1|^{-1} , \qquad \hat{c}_2 = |\Lambda_{01}|^{-1} - |\Lambda_1 \Lambda_0|^{-1} \\
\hat{c}_3 &= |\Lambda_{001}|^{-1} - |\Lambda_0 \Lambda_{01}|^{-1} + |\Lambda_{011}|^{-1} - |\Lambda_{01} \Lambda_1|^{-1}
\end{aligned}$$

etc.. Using the cycles up to length 6 we get

$$\begin{aligned}
1/\zeta(z) &= 1 - 0.416667z - 0.00833333z^2 \\
&\quad +0.000079446z^3 - 9.89291 \times 10^{-7} z^4 + \ldots
\end{aligned}$$

The leading zero of this Taylor series is an estimate of $\exp(\gamma)$. *Using* $n = 1$, *2, 3 and 4 we obtain the increasingly accurate estimates for* γ: *0.875469, 0.830597, 0.831519 and 0.831492 In a hope to improve the convergence we can use the Padé approximates* $P^N_M(z) = \sum_{i=1}^N p_i z^i / (1 + \sum_{j=1}^M q_j z^j)$. *Using the Padé approximates* $P^{n-1}_1(z)$ *for* $n = 2$, *3 and 4 we obtain the estimates 0.828585, 0.831499 and 0.831493.*

The above results correspond to $A = 6$; *in the* $A = 9/2$ *case the leading zero is* $1/z = 1.43549\ldots$ *and* $\gamma = 0.36150\ldots$. *(Adam Prügel-Bennet)*

Solution 18.2: Spectral determinant for a 1-d repeller *We are told the correct expression for the escape rate is also given by the logarithm of the leading zero of the spectral determinant (15.12), expanded as the Taylor series (18.8). The coefficients* c_i *should fall off super-exponentially so that truncating the Taylor series is expected to give a far more accurate estimate of the escape rate than using the dynamical zeta function. How do we compute the* c_i *coefficients in (18.8)? One straightforward method is to first compute the Taylor expansion of* $\log(F(z))$

$$\begin{aligned}
\log(F(z)) &= \sum_p \sum_{k=0} \log\left(1 - \frac{t_p}{\Lambda_p^k}\right) = -\sum_p \sum_{k=0} \sum_{r=1} \frac{t_p^r}{\Lambda_p^{kr}} \\
&= -\sum_p \sum_{r=1} \frac{t_p^r}{1 - \Lambda_p^{-r}} = -\sum_p \sum_{r=1} B_p(r) z^{n_p r}
\end{aligned}$$

where $B_p(r) = -1/r|\Lambda_p^r|(1+\Lambda_p^{-r})$ *. Writing* $\log(F(z))$ *as a power series*

$$\log(F(z)) = -\sum_{i=1} b_i z^i$$

we obtain

$$\begin{aligned}
b_1 &= B_0(1) + B_1(1) \\
b_2 &= B_{01}(1) + B_0(2) + B_1(2) \\
b_3 &= B_{001}(1) + B_{011}(1) + B_0(3) + B_1(3) \\
b_3 &= B_{0001}(1) + B_{0011}(1) + B_{0111}(1) + B_{01}(2) + B_0(4) + B_1(4) \qquad \text{(R.62)}
\end{aligned}$$

etc.. To obtain the coefficients for the spectral determinant we solve

$$F(z) = 1 - \sum_{i=1} Q_i z^i = \exp\left(\sum_{i=1} b_i z^i\right)$$

for the Q_i*'s. This gives*

$$\begin{aligned}
Q_1 &= b_1 \,, \quad Q_2 = b_2 + b_1^2/2 \,, \quad Q_3 = b_3 + b_1 b_2 + b_1^3/6 \\
Q_4 &= b_4 + b_1 b_3 + b_2^2/2 + b_2 b_1^2/2 + b_1^4/24
\end{aligned}$$

Using these formulas we find

$$F(z) = 1 - 0.4z - 0.0152381z^2 - 0.0000759784z^3 + 4.5311 \times 10^{-9} z^4 + \cdots$$

The logarithm of the leading zero of $F(z)$ *again gives the escape rate. Using the* $n = 1$*, 2, 3, and 4 truncations we find the approximation to* γ *of 0.916291, 0.832345, 0.83149289 and 0.8314929875. As predicted, the convergence is much faster for the spectral determinant than for the dynamical zeta function.*

In figure R.9 we show a plot of the logarithm of the coefficients for the spectral determinant and for the dynamical zeta function.

(Adam Prügel-Bennet)

The above results correspond to $A = 6$*; in the* $A = 9/2$ *case all cycles up to length 10 yield* $\gamma = 0.36150966984250926\ldots$*. (Vadim Moroz)*

Solution 18.2: Escape rate for a 1-d repeller *We can compute an approximate functional dependence of the escape rate on the parameter* a *using the stabilities of the first five prime orbits computed above, see (R.61). The spectral determinant (for* $a > 4$*) is*

$$\begin{aligned}
F &= 1 - \frac{2z}{a-1} - \frac{8z^2}{(a-3)(a-1)^2(a+1)} \\
&\quad + \left(\frac{2(32 - 18a + 17a^2 - 16a^3 + 14a^4 - 6a^5 + a^6)}{(a-3)(a-1)^3(1+a)(a^2-5a+7)(a^2+a+1)} \right. \qquad \text{(R.63)} \\
&\qquad \left. - \frac{2a(a-2)\sqrt{(a^2-2a-7)}}{(a^2-5a+7)(a^2-2a-7)(a^2+a+1)} \right) z^3
\end{aligned}$$

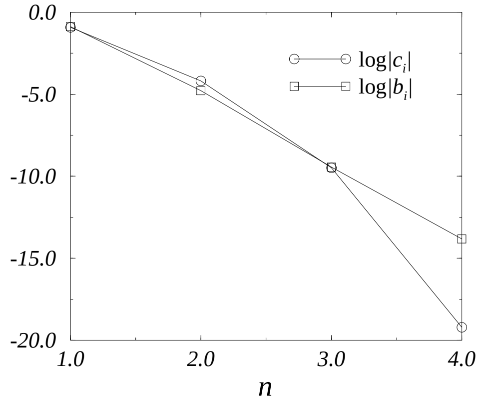

Figure R.9: Plot of the Taylor coefficients for the spectral determinant, c_i, and for the dynamical zeta function, b_i.

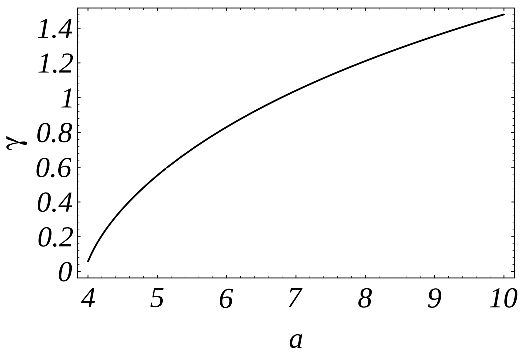

Figure R.10: Plot of the escape rate versus a for the logistic map $x_{n+1} = ax_n(1-x_n)$ calculated from the first five periodic orbits.

evaluate this at $a = 6$ to see how good it is? I guess already know...

The leading zero is plotted in figure R.10; it always remains real while the other two roots which are large and negative for $a > 5.13\ldots$ become imaginary below this critical value. The accuracy of this truncation is clearly worst for $a \to 4$, the value at which the hyperbolicity is lost and the escape rate goes to zero.

(Adam Prügel-Bennet)

Solution 18.4: Escape rate for the Ulam map. *The answer is worked out in* Nonlinearity **3**, *325;* **3**, *361 (1990).*

give exact page number

Chapter 19

Solution 19.3:

(d) *In the $A = 9/2$ case all cycles up to length 9 yield $\lambda = 1.08569\ldots$. (Vadim Moroz)*

Solution 9.4: *The escape rate is the leading zero of the zeta function*

$$0 = 1/\zeta(\gamma) = 1 - e^{\gamma}/2a - e^{\gamma}/2a = 1 - e^{\gamma}/a.$$

So, $\gamma = \log(a)$ *if* $a > a_c = 1$ *and* $\gamma = 0$ *otherwise. For* $a \approx a_c$ *the escape rate behaves like*

$$\gamma(a) \approx (a - a_c).$$

Solution 19.1: *The escape is controlled by the size of the primary hole of the repeller. All subholes in the repeller will be proportional with the main hole. The size of the main hole is* $l = \sqrt{1 - 1/a}$. *Near* $a_c = 1$ *the escape rate is*

$$\gamma(a) \sim (a - a_c)^{1/2}.$$

We can generalize this and the previous result and conclude that

$$\gamma(a) \sim (a - a_c)^{1/z},$$

where z *is the order of the maximum of the single humped map.*

Solution 19.2: *By direct evaluation we can calculate the zeta functions and the Fredholm determinant of this map. The zeta functions are*

$$1/\zeta_k(z) = \det(1 - z\mathbf{T}_k),$$

where

$$\mathbf{T}_k = \begin{pmatrix} T_{00}^{k+1} & T_{01}^{k+1} \\ T_{10}^{k+1} & T_{11}^{k+1} \end{pmatrix},$$

and $T_{00} = 1/a_1$, $T_{01} = (b - b/a_1)/(1 - b)$, $T_{11} = (1 - b - b/a_2)/(1 - b)$, $T_{10} = 1/a_2$ *are inverses of the slopes of the map. The Fredholm determinant is the product of zeta functions*

$$F(z) = \prod_{k=0}^{\infty} 1/\zeta_k(z).$$

The leading zeroes of the Fredholm determinant can come from the zeroes of the leading zeta functions.

The zeroes of $1/\zeta_0(z)$ *are*

$$\begin{aligned} 1/z_1 &= \tfrac{T_{00}+T_{11}+\sqrt{(T_{00}-T_{11})^2+4T_{01}T_{10}}}{2}, \\ 1/z_2 &= \tfrac{T_{00}+T_{11}-\sqrt{(T_{00}-T_{11})^2+4T_{01}T_{10}}}{2}. \end{aligned}$$

The zeroes of $1/\zeta_1(z)$ *are*

$$\begin{aligned} 1/z_3 &= \tfrac{T_{00}^2+T_{11}^2+\sqrt{(T_{00}^2-T_{11}^2)^2+4T_{01}^2T_{10}^2}}{2}, \\ 1/z_4 &= \tfrac{T_{00}^2+T_{11}^2-\sqrt{(T_{00}^2-T_{11}^2)^2+4T_{01}^2T_{10}^2}}{2}. \end{aligned}$$

By substituting the slopes we can show that $z_1 = 1$ *is the leading eigenvalue. The next to leading eigenvalue, which is the correlation decay in discrete time, can be* $1/z_3$ *or* $1/z_2$.

Chapter 20

1

Solution 20.1: *In the higher dimensional case there is no change in the derivation except Λ_p should be replaced with the product of expanding eigenvalues $\prod_j |\Lambda_{p,j}|$. The logarithm of this product is $\sum_j \log |\Lambda_{p,j}|$. The average of $\log |\Lambda_{,j}|$ is the j-th Lyapunov exponent.*

Solution 20.4: *The zeta function for the two scale map is*

$$1/\zeta(z,\beta) = 1 - z\left(\frac{1}{a^\beta} + \frac{1}{b^\beta}\right).$$

The pressure function is

$$P(\beta) = \log z_0(\beta) = -\log\left(\frac{1}{a^\beta} + \frac{1}{b^\beta}\right).$$

The escape rate is

$$\gamma = P(1) = -\log\left(\frac{1}{a} + \frac{1}{b}\right),$$

The topological entropy is

$$K_0 = h_{top} = -P(0) = \log 2.$$

The Lyapunov exponent is

$$\overline{\lambda} = P'(1) = \frac{\log a/a + \log b/b}{1/a + 1/b}.$$

The Kolmogorov entropy is

$$K_1 = \overline{\lambda} - \gamma = P'(1) - P(1) = \frac{\log a/a + \log b/b}{1/a + 1/b} + \log\left(\frac{1}{a} + \frac{1}{b}\right).$$

The Rényi entropies are

$$K_\beta = (P(\beta) - \beta\gamma)/(\beta - 1) = (\log\left(\frac{1}{a^\beta} + \frac{1}{b^\beta}\right) + \beta\log\left(\frac{1}{a} + \frac{1}{b}\right))/(1-\beta).$$

The box counting dimension is the solution of the implicit equation $P(D_0) = 0$, which is

$$1 = \frac{1}{a^D_0} + \frac{1}{b^D_0}.$$

The information dimension is

$$D_1 = 1 - \gamma/\overline{\lambda}.$$

The rest of the dimensions can be determined from equation $P(q-(q-1)D_q) = \gamma q$. Taking $\exp$ of both sides we get

$$\frac{1}{a^{q-(q-1)D_q}} + \frac{1}{b^{q-(q-1)D_q}} = \left(\frac{1}{a} + \frac{1}{b}\right)^q.$$

For a given q we can find D_q from this implicit equation.

[1]Vattay: I could not find a solution file to exerThermo. Somebody who wrote the original exercises might have a soluton to the first 3 problems and can add it to soluThermo.tex .

Solution 20.5: *The zeta function is*

$$1/\zeta(z,\beta) = \det(1 - \mathbf{T}_{\beta-1}),$$

where we replaced k with $\beta - 1$ in solution R. The pressure can be calculated from the leading zero which is (see solution R)

$$P(\beta) = \log z_0(\beta) = -\log\left(\frac{T_{00}^\beta + T_{11}^\beta + \sqrt{(T_{00}^\beta - T_{11}^\beta)^2 + 4T_{01}^\beta T_{10}^\beta}}{2}\right).$$

Solution 20.6: *We can easily read off that $b = 1/2$, $a_1 = arcsin(1/2)/2\pi$ and $a_2 = a_1$ and do the steps as before.*

Chapter 21

(No solutions available.)

Chapter 22

(No solutions available.)

Chapter 23

Solution 23.1: Diffusion for odd integer Λ. *Consider first the case $\Lambda = 3$, illustrated in figure R.11. If $\beta = 0$, the dynamics in the elementary cell is simple enough; a partition can be constructed from three intervals, which we label $\{\mathcal{M}_1, \mathcal{M}_2, \mathcal{M}_3\}$, with the alphabet ordered as the intervals are laid out along the unit interval. The Markov graph is figure R.11(c), and the dynamical zeta function is*

$$1/\zeta|_{\beta=0} = 1 - (t_1 + t_2 + t_3) = 1 - 3z/\Lambda\,,$$

with eigenvalue $z = 1$ as required by the flow conservation.

However, description of global diffusion requires more care. As explained in the definition of the map (23.9), we have to split the partition $\mathcal{M}_2 = \mathcal{M}_4 \cup (\frac{1}{2}) \cup \mathcal{M}_5$, and exclude the fixed point $f(\frac{1}{2}) = \frac{1}{2}$, as the map $\hat{f}(\hat{x})$ is not defined at $\hat{f}(\frac{1}{2})$. (Are we to jump to the right or to the left at that point?) As we have $f(\mathcal{M}_4) = \mathcal{M}_1 \cup \mathcal{M}_4$, and similarly for $f(\mathcal{M}_5)$, the Markov graph figure R.11(d) is infinite, and so is the dynamical zeta function:

$$1/\zeta = 1 - t_1 - t_{14} - t_{144} - t_{1444}\cdots - t_3 - t_{35} - t_{355} - t_{3555}\cdots.$$

The infinite alphabet $\mathcal{A} = \{1, 14, 144, 1444\cdots 3, 35, 355, 3555\cdots\}$ is a consequence of the exclusion of the fixed point(s) x_4, x_5. As is customary in such situations (see sect. 21.3.1, *exercise 18.11, and chapter 21,* inter alia*), we deal with this by dividing*

⇓PRELIMINARY
⇑PRELIMINARY

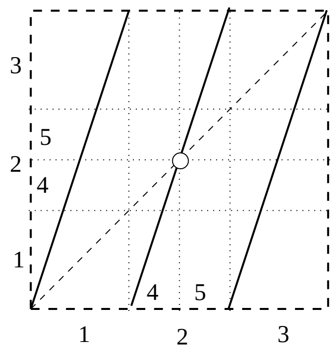

(a) **(b)** **(c)** **(d)**

Figure R.11: (a) (b) A partition of the unit interval into three or five intervals, labeled by the order along the unit interval $\mathcal{A} = \{\mathcal{M}_1, \mathcal{M}_2 = \mathcal{M}_4 \cup (\frac{1}{2}) \cup \mathcal{M}_5, \mathcal{M}_3\}$. The partition is Markov, as the critical point is also a fixed point. (c) the Markov graph for this Markov partition.

out the undesired fixed point from the dynamical zeta function. We can factorize and resum the weights using the piecewise linearity of (23.9)

$$1/\zeta = 1 - \frac{t_1}{1-t_4} - \frac{t_3}{1-t_5} \,.$$

The diffusion constant is now most conveniently evaluated by evaluating the partial derivatives of $1/\zeta$ as in (18.16)

$$\begin{aligned} \langle T \rangle_\zeta &= -z\frac{\partial}{\partial z}\frac{1}{\zeta} = 2\left(\frac{t_1}{1-t_4} + \frac{t_1 t_4}{(1-t_4)^2}\right)\Bigg|_{z=1,\beta=0} = \frac{3}{4} \\ \left\langle \hat{x}^2 \right\rangle_\zeta\Big|_{z=1,\beta=0} &= 2\left(\frac{\hat{n}_1(\hat{n}_1+\hat{n}_4)\Lambda^2}{(1-1/\Lambda)^2} + 2\frac{\hat{n}_4^2/\Lambda^3}{(1-1/\Lambda)^3}\right) = \frac{1}{2} \end{aligned} \qquad (R.64)$$

yielding $D = 1/3$, in agreement with in (23.21) for $\Lambda = 3$.

Chapter 25

(No solutions available.)

Chapter 29

Solution 29.2: Green's function. *The Laplace transform of the (time-dependent) quantum propagator*

$$K(q, q', t) = \sum_n \phi_n(q) e^{-iE_n t/\hbar} \phi_n^*(q')$$

is the (energy-dependent) Green's function

$$G(q, q', E + i\varepsilon) = \frac{1}{i\hbar}\int_0^\infty dt\; e^{\frac{i}{\hbar}Et - \frac{\varepsilon}{\hbar}t} \sum_n \phi_n(q) e^{-iE_n t/\hbar} \phi_n^*(q')$$

$$
\begin{aligned}
&= \frac{1}{i\hbar}\sum_n \phi_n(q)\phi_n^*(q')\int_0^\infty dt\; e^{\frac{i}{\hbar}(E-E_n+i\varepsilon)t} \\
&= -\sum_n \phi_n(q)\phi_n^*(q')\frac{1}{E-E_n+i\varepsilon}e^{-\frac{\varepsilon}{\hbar}t}e^{i(E-E_n)t/\hbar}\Big|_{t=0}^{t=\infty} .
\end{aligned}
$$

Dirac delta function
delta function!Dirac

When ε is positive, $e^{-\frac{\varepsilon}{\hbar}\infty} = 0$, so

$$
G(q,q',E+i\varepsilon) = \sum_n \frac{\phi_n(q)\phi_n^*(q')}{E-E_n+i\varepsilon} .
$$

(Bo Li)

Solution 29.1: Lorentzian representation of the Dirac delta function. *General hint: read up on principal parts, positive and negative frequency parts of the Dirac delta function, perhaps the Cauchy theorem, in any good quantum mechanics textbook.*

To see that (29.19) satisfies properties of the delta function,

$$
\delta(E-E_n) = -\lim_{\varepsilon\to 0}\frac{1}{\pi}\mathrm{Im}\,\frac{1}{E-E_n+i\varepsilon} ,
$$

start by expressing explicitely the imaginary part:

$$
\begin{aligned}
-\mathrm{Im}\,\frac{1}{E-E_n+i\varepsilon} &= -\mathrm{Im}\,\frac{E-E_n-i\varepsilon}{(E-E_n+i\varepsilon)(E-E_n-i\varepsilon)} \\
&= \frac{\varepsilon}{(E-E_n)^2+\varepsilon^2} .
\end{aligned}
$$

This is a Lorenzian of width ϵ, with a peak at $E=E_n$. It has the correct normalization for the delta function,

$$
\begin{aligned}
\frac{1}{\pi}\int_{-\infty}^{\infty} dE \frac{\varepsilon}{(E-E_n)^2+\varepsilon^2} &= \frac{1}{\pi}\frac{\varepsilon}{\varepsilon}\arctan\frac{E-E_n}{\varepsilon}\Big|_{-\infty}^{\infty} \\
&= \frac{1}{\pi}(\pi/2-(-\pi/2)) \;=\; 1 ,
\end{aligned}
$$

so

$$
\frac{1}{\pi}\int_{-\infty}^{\infty} dE \frac{\epsilon}{(E-E_n)^2+\epsilon^2} = 1 , \tag{R.65}
$$

independently of the width ϵ.

Next we show that in the $\epsilon\to\infty$ limit the support of the Lorentzian is concentrated at $E=E_n$. When $E=E_n$,

$$
\lim_{\varepsilon\to 0}\frac{1}{\pi}\left(\frac{\varepsilon}{(E-E_n)^2+\varepsilon^2}\right) = \lim_{\varepsilon\to 0}\frac{1}{\pi}\frac{1}{\varepsilon} = \infty ,
$$

and when $E \neq E_n$,

$$\lim_{\varepsilon\to 0}\frac{1}{\pi}\frac{\varepsilon}{(E-E_n)^2+\varepsilon^2}=0$$

Providing that a function convolved with $\delta(s)$, $\int f(E)\delta(E-E_n)dE$ has a continuous first derivative at $E = E_n$ and falls of sufficiently rapidly as $E \to \pm\infty$, this is a representation of the delta function.

(R. Paskauskas, Bo Li)

Chapter 30

Solution 30.2: Fresnel integral. *Start by re-expressing the integral overthe infinite half-line:*

$$\frac{1}{\sqrt{2\pi}}\int_{-\infty}^{\infty} dx\, e^{-\frac{x^2}{2ia}} = \frac{2}{\sqrt{2\pi}}\int_0^{\infty} dx\, e^{-\frac{x^2}{2ia}}\,, \qquad a\in\mathbb{R}\,,\quad a\neq 0\,.$$

When $a > 0$, the contour 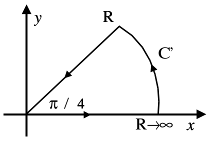 *vanishes, as it contains no pole:*

$$\begin{aligned}\oint_C dz\, e^{-z^2/2ia} &= \int_0^{\infty} dx\, e^{-\frac{x^2}{2ia}} + \int_{C'} + \int_{\infty}^{0} e^{i\frac{\pi}{4}} e^{-\frac{x^2}{2a}}\, dx = 0\\ \int_{C'} &= \int_0^{\frac{\pi}{4}} e^{iR^2 e^{i2\phi}/2a} R e^{i\phi} i d\phi = 0\,. \end{aligned} \tag{R.66}$$

So

$$\frac{2}{\sqrt{2\pi}}\int_0^{\infty} dx\, e^{-\frac{x^2}{2ia}} = \frac{2}{\sqrt{2\pi}}\int_0^{\infty} dx\, e^{i\frac{\pi}{4}} e^{-\frac{x^2}{2a}} = e^{i\frac{\pi}{4}}\sqrt{a} = \sqrt{ia}$$

In the $a < 0$ case take the contour 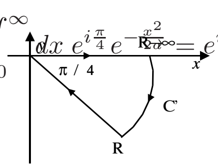

$$\begin{aligned}\oint_C dz\, e^{-z^2/2ia} &= \int_0^{\infty} dx\, e^{-\frac{x^2}{2ia}} + \int_{C'} + \int_{\infty}^{0} e^{-i\frac{\pi}{4}} e^{\frac{x^2}{2a}}\, dx\\ &= \int_0^{\infty} dx\, e^{-\frac{x^2}{2ia}} - e^{-i\frac{\pi}{4}}\int_0^{\infty} dx\, e^{\frac{x^2}{2a}} = 0\,.\end{aligned}$$

Again

$$\frac{2}{\sqrt{2\pi}}\int_0^{\infty} dx\, e^{-\frac{x^2}{2ia}} = e^{-i\frac{\pi}{4}}\sqrt{|a|}\,,$$

and, as one should have perhaps intuited by analyticity arguments, for either sign of a we have the same Gaussian integral formula

$$\frac{1}{\sqrt{2\pi}}\int_{-\infty}^{\infty} dx\, e^{-\frac{x^2}{2ia}} = |a|^{1/2} e^{i\frac{\pi}{4}\frac{a}{|a|}} = \sqrt{ia}\,.$$

The vanishing of the C' contour segment (R.66) can be proven as follows: Substitute $z = Re^{i\phi}$ into the integral

$$I_R = \int_0^{\frac{\pi}{4}} e^{iR^2 e^{i2\phi}/2a} Re^{i\phi} i d\phi = \int_0^{\frac{\pi}{4}} e^{iR^2(\cos 2\phi + i \sin 2\phi)/2a} Re^{i\phi} i d\phi \,.$$

Then

$$|I_R| \le R \int_0^{\frac{\pi}{4}} e^{-R^2 \sin 2\phi/2a} d\phi = \frac{R}{2} \int_0^{\frac{\pi}{2}} e^{-R^2 \sin\theta/2a} d\theta \,.$$

In the range $[0, \pi/2]$ we can replace $\frac{2}{\pi}\theta \le \sin\theta$, obtain a bound

$$|I_R| \le \frac{R}{2} \int_0^{\frac{\pi}{2}} e^{-R^2\theta/\pi a} d\theta = \frac{R}{2} \frac{1 - e^{-R^2/2a}}{R^2/a\pi} \,,$$

so

$$\lim_{R\to\infty} |I_R| = 0 \,.$$

(Bo Li)

Chapter 31

Solution 31.7: Free particle R-function. *Calculate R by its definition*

$$R(q', q, t) = \int_0^t \mathcal{L}(\dot{q}(t'), q(t'), t') dt'$$

where the solution of Lagrange equations of motion is substituted for $q(t)$.

a) *a D-dimensional free particle:*
   We have
   $\mathcal{L}(\dot{q}(t'), q(t'), t') = \frac{m}{2} \sum_{i=1}^{D} [\dot{q}_i(t')]^2$,
   $\dot{q}_i(t) = \mathrm{const} = \frac{q_i' - q_i}{t}$.
   Answer:
   $R(q', q, t) = \frac{m}{2} \sum_{i=1}^{D} \frac{[q_i' - q_i]^2}{t}$.
b) *Using symmetric gauge for vector potential and denoting the Larmor frequency by $\omega = \frac{eB}{mc}$, we have*

   $$\mathcal{L} = \frac{m}{2}\left(\dot{x}^2 + \dot{y}^2 + \dot{z}^2 + \omega(x\dot{y} - y\dot{x})\right)$$

   The equations of motion are
   $\ddot{x} - \omega\dot{y} = 0$,
   $\ddot{y} + \omega\dot{x} = 0$,
   $\ddot{z} = 0$.

To calculate the expression for the principal function we do integration by parts on $\dot{x}^2 + \dot{y}^2$, and the result is

$$R = \int \mathcal{L} dt = \frac{m}{2} \left(x\dot{x}|_{t_0}^t + y\dot{y}|_{t_0}^t + \frac{(z' - z)^2}{t} + \int_{t_0}^t \left[x(-\ddot{x} + \omega\dot{y}) + y(-\ddot{y} - \omega\dot{x}) \right] dt \right),$$

however terms inside the integral vanish by equations of motion. Denote $w(t) = x(t) + \imath y(t)$, then the first two equations of motion are equivalent to equation in complex $w(t)$:

$$\ddot{w}(t) + \imath\omega\dot{w}(t) = 0$$

Solution to which is

$$w' \equiv w(t) = w + \frac{\dot{w}(1 - e^{-\imath\omega t})}{\imath\omega}$$

We must reexpress velocities in R in terms of time and initial and final coordinates. In terms of $\dot{w}$ we have

$$\dot{w}_0 = \frac{\omega}{2} \frac{e^{\frac{\imath\omega t}{2}}(w - w_0)}{\sin(\frac{\omega t}{2})}$$

$$\dot{w} = \frac{\omega}{2} \frac{e^{\frac{-\imath\omega t}{2}}(w - w_0)}{\sin(\frac{\omega t}{2})}$$

Notice that

$$x\dot{x} + y\dot{y} = \mathrm{Re}\, w^* \dot{w}$$

$$\mathrm{Re}\, w^* \dot{w}|_0^t = \frac{\omega}{2\sin\frac{\omega t}{2}} \left((|w|^2 + |w_0|^2)\cos\frac{\omega t}{2} - 2\mathrm{Re}\, w_0 w^* e^{\frac{-\imath\omega}{2}} \right)$$
$$= \frac{\omega}{2} \left(\cot(\tfrac{\omega t}{2})[(x - x_0)^2 + (y - y_0)^2] + 2(x_0 y - y_0 x) \right)$$
$$R = \frac{m(z-z_0)^2}{2t} + \frac{m\omega}{4} \left(\cot(\tfrac{\omega t}{2})[(x - x_0)^2 + (y - y_0)^2] + 2(x_0 y - y_0 x) \right)$$

c)

Solution 31.2: Dirac delta function, Gaussian representation. *To prove that δ_σ converges to a dirac delta function, it is enough to show that it has the following properties:*

1. $\int_{-\infty}^{\infty} \delta_\sigma(x) dx = 1$
2. $\lim_{\sigma\to 0} \int_{-a}^{a} f(x)\delta_\sigma(x) dx$=*f(0)*

for arbitrary $f(x)$ continuous and positive a.

First property is satisfied by the choise of normalisation constant.

Second property is verified by the change of variables $y = x/\sqrt{2\sigma^2}$:

$$\lim_{\sigma\to 0} \int_{-a}^{a} f(x)\delta_\sigma(x) dx = \lim_{\sigma\to 0} \frac{1}{\sqrt{\pi}} \int_{\frac{-a}{\sqrt{2\sigma^2}}}^{\frac{a}{\sqrt{2\sigma^2}}} f(\sqrt{2\sigma^2} y) e^{-y^2} dy = f(0)$$

(Rytis Paškauskas)

stationary!phase approximation

Solution 31.3: d-dimensional Gaussian integrals.

We require that the matrix in the exponent is nondegenerate (i.e. has no zero eigenvalues.) The converse may happen when doing stationary phase approximations which requires going beyond the Gaussian saddlepoint approximation, typically to the Airy-function type stationary points [30.10]. We also assume that M is positive-definite, otherwise the integral is infinite.

Make a change of variables $y = Ax$ such that $A^T M^{-1} A = \mathrm{Id}$. Then

$$I = \frac{1}{(2\pi)^{d/2}} \int_{\mathbf{R}^d} \exp[-\frac{1}{2}\sum_i (y_i^2 - 2(JA)_i y_i)] |\det A| dy$$

Complete each term under in the sum in the exponent to a full square

$$y_i^2 - 2(JA)_i y_i = (y_i - (JA)_i)^2 - (JA)_i^2$$

and shift the origin of integration to $JA/2$, so that

$$I = \frac{1}{(2\pi)^{d/2}} \exp(\frac{1}{2} J^T A A^T J) |\det A| \int_{\mathbf{R}^d} \exp[-\frac{1}{2}\sum_i y_i^2] dy$$

Note that $AA^T M^{-1} AA^T = AA^T$, therefore $AA^T = M$ and $|\det A| = \sqrt{\det M}$. The remaining integral is equal to a Poisson integral raised to the d-th power, i.e. $(2\pi)^{d/2}$. Answer:

$$I = \sqrt{\det M} \exp[\frac{1}{2} J^T M J]$$

(Rytis Paškauskas)

Solution 31.4: Stationary phase approximation.

Main contribution to this integral come from critical points of $\Phi(x)$. Suppose that p is such a nondegenerate critical point, $p : D\Phi(p) = 0$, and $D^2\Phi(p)$ has full rank. Then there is a local coordinate system y in the neighbourhood of p such that $\Phi(p+y) = \Phi(p) - \sum_{i=1}^{\lambda} y_i^2 + \sum_{i=\lambda+1}^{d} y_i^2$, where λ is the number of negative eigenvalues of $D^2\Phi(p)$. Indeed, if we set $x - p = Ay$, then $\Phi(x) \approx \Phi(p) + \frac{1}{2} y A^T D^2\Phi(p) A y$. There exist such A that $\frac{1}{2} A^T D^2\Phi(p) A = \mathrm{diag}[\underbrace{-1, \ldots -1}_{\lambda}, \underbrace{+1, \ldots}_{d-\lambda}]$. With this change of variables in mind, we have

$$I = e^{\frac{\iota\Phi(p)}{\hbar}} \int_{\mathrm{R}^d} e^{\frac{\iota}{\hbar}(-\sum_{i=1}^{\lambda} y_i^2 + \sum_{i=\lambda+1}^{d} y_i^2)} |\det A| dy = e^{\frac{\iota\Phi(p)}{\hbar}} (\pi\hbar)^{d/2} e^{\frac{\iota\pi}{4}(-2\lambda+d)} |\det A|$$

Furthermore, $(\det A)^2 \det D^2\Phi(p) = 2^d \exp \iota\pi\lambda$, therefore

$$|\det A| = \frac{2^{d/2} \exp\frac{\iota\pi\lambda}{2}}{\sqrt{\det D^2\Phi(p)}}.$$

stationary!phase approximation

Phase factors $\exp \iota\pi\lambda/2$ *and* $\exp -\iota\pi\lambda/2$ *cancel out. Substitute* $\exp \iota\pi d/2 = \iota^{d/2}$.

The result:

$$I = \frac{(2\iota\pi\hbar)^{d/2} e^{\frac{\iota\Phi(p)}{\hbar}}}{\sqrt{\det D^2\Phi(p)}}$$

Critical nondegenerate points are isolated. Therefore if Φ *has more than one critical point, then equivalent local approximation can be made in the neighbourhoods of each critical point and the complete approximation to the integral made by adding contributions of all critical points.*

Answer:

$$I = \sum_{p:D\Phi(p)=0} \frac{(2\iota\pi\hbar)^{d/2} e^{\frac{\iota\Phi(p)}{\hbar}} A(p)}{\sqrt{\det D^2\Phi(p)}}$$

Rytis Paškauskas

Solution 31.4: Stationary phase approximation.

values of x *of stationary phase, the points for which the gradient of the phase vanishes*

$$\frac{\partial}{\partial x}\Phi(x) = 0.$$

Intuitively, these are the important contributions as for $\hbar \to 0$ *the phase* $\Phi(x)/\hbar$ *grows large and the function* $e^{i\Phi(x)/\hbar}$ *oscillates rapidly as a function of* x*, with the negative and positive parts cancelling each other. More precisely, if the stationary points are well separated local extrema of* $\Phi(x)$*, we can deform the integration contour and approximate* $\Phi(x)/\hbar$ *up to the second order in* x *by*

$$I \approx \sum_n A(x_n) e^{i\Phi(x_n)/\hbar} \int d^d x e^{\frac{i}{2\hbar}(x-x_n)^T \mathbf{D^2}\Phi(x_n)(x-x_n)}.$$

The second derivative matrix is a real symmetric matrix, so we can transform it to a diagonal matrix by a similarity transformation

$$\mathit{Diag}(\lambda_1, ..., \lambda_d) = \mathbf{O}\mathbf{D}^2\Phi\mathbf{O}^+ ,$$

where $\mathbf{O}$ *is a matrix of an orthogonal transfomation. In the rotated coordinate system* $u = \mathbf{O}(x - x_n)$ *and the integral takes form*

$$I \approx \sum_n A(x_n) e^{i\Phi(x_n)/\hbar} \int d^d u e^{\sum_{k=1}^d i\lambda_k u_k^2/2\hbar} ,$$

where we used the fact that the Jacobi determinant of an orthogonal transformation is $\det \mathbf{O} = 1$. *Carrying out the Gauss integrals*

stationary!phase approximation

$$\int du e^{i\lambda u^2/2\hbar} = \frac{(2\pi i\hbar)^{1/2}}{\sqrt{\lambda}} \tag{R.67}$$

and using $\det \mathbf{D}^2\Phi(x_n) = \prod_{k=1}^{d} \lambda_k$ *we obtain the stationary phase estimate of (31.55).*

A nice exposition of the subject is given in ref. [30.10].

Solution 33.2: Stationary phase approximation in higher dimensions. *In this case* $1/\hbar$ *is assumed to be a very large number. parameter. The idea of this method is that we only evaluate part of integral* I *where* $e^{i\varphi}$ *is stationary that is,* $\varphi \approx$*const. That means we need extrema (saddle points) of manifold* Φ. *In this case*

$$\frac{\partial \Phi}{\partial x_{sp,\mu}} = 0$$

Introduce a new d*-dimensional variable* s *such, that*

$$i\Phi(x) = i\Phi(x_{sp,\mu}) - s^2$$

Integral I *in terms of new variables is*

$$I = \sum_n e^{i\Phi(x_n)/\hbar} \int e^{-s^2/\hbar} A(x_n(s)) \left|\frac{Dx}{Ds}\right| d^d s$$

Here n *sums all stationary phase points which the path of integration (in complex plane!) meets. next, we need to calculate the Jacobian* J*:*

$$J = 1/\left|\frac{\partial s_i}{\partial x_k}\right|,$$

where

$$\frac{\partial s_i}{\partial x_k} = \frac{1}{2is_i}\frac{\partial \Phi}{\partial x_k}.$$

This expression is undetermined at stationary phase points, because its right hand side becomes division zero by zero. However, by the chain rule

$$\frac{\partial s_i}{\partial x_k} = \frac{1}{2i\frac{\partial s_i}{\partial x_m}} \frac{\partial \Phi^2}{\partial x_k \partial x_m}$$

where $x = x_{sp}$ *are evaluated at the stationary phase point. From this expression we obtain that*

$$\left[\left(\frac{\partial s}{\partial x}\right)^2\right]_{i,k} = \frac{1}{2i}\frac{\partial \Phi^2}{\partial x_i \partial x_k}$$

So the Jacobian is (employing a standard notation for a second derivative)

$$J = \frac{(2i)^{d/2}}{\sqrt{\det D^2\Phi}} \,.$$

Since the exponential factor $e^{-s^2/\hbar}$ cuts integration sharply because of a very large parameter $1/\hbar$, the function is evaluated only at the stationary point $s = 0$, and the integral is approximately

$$I \approx \sum_n e^{i\Phi(x_n)/\hbar} A(x_n) \frac{(2i)^{d/2}}{\sqrt{\det D^2\Phi(x_n)}} \int e^{-s^2/\hbar} d^d s$$

Limits of integration may depend on particular situation. If limits are infinite, then

$$\int e^{-s^2/\hbar} d^d s = \left(\int_{-\infty}^{\infty} e^{-s^2/\hbar} ds \right) = (\pi\hbar)^{d/2}$$

We substitute this into I and get the answer.

(Rytis Paškauskas)

Solution 31.13: D-dimensional free particle propagator. *A free particle reachs q from q' by only one trajectory. Taking this into account the semiclassical Van Vleck propagator is*

$$K_{sc}(q, q', t) = \frac{e^{\frac{iR}{\hbar}}}{(2\pi i\hbar)^{d/2}} \left| \det \frac{\partial^2 R}{\partial q_i \partial q'_j} \right|^{1/2}$$

The principal function of free motion in D-dimensions is

$$R(q, q', t) = \frac{m}{2t} \sum_{\mu=1}^{D} (q_\mu - q'_\mu)^2$$

The derivative is

$$\frac{\partial^2 R}{\partial q_i \partial q'_j} = -\delta_{i,j} \frac{m}{t}$$

According to that determinant is

$$\left| \det \frac{\partial^2 R}{\partial q_i \partial q'_j} \right|^{1/2} = e^{i\pi D/2} \left(\frac{m}{t} \right)^{D/2} \,,$$

and the Van Vleck propagator is

$$K_{sc}(q, q', t) = e^{i\pi D/4} \left(\frac{m}{2\pi\hbar t} \right)^{D/2} \prod_{\mu=1}^{D} \exp\left[\frac{im}{2\hbar t} \left(q_\mu - q'_\mu \right)^2 \right]$$

The next step is to calculate the exact quantum propagator:

$$K(q,q',t) = \sum_n \phi_n(q) e^{-iE_n t/\hbar} \phi_n^*(q')$$

Taking that particle wave function in free space is

$$\phi_p(q) = \frac{1}{(2\pi\hbar)^{D/2}} e^{ipq/\hbar}$$

we derive that propagator K is

$$\frac{1}{(2\pi\hbar)^D} \int e^{-\frac{it}{2m\hbar}p^2 + ip(q-q')} d^D p$$

We can split multi-dimensional integral that stands here into a product of one dimensional integrals. Then we should change variables for purpose of reduction to Poisson-type integrals. We have omitted some straightforward algebra. The result is that the semiclassical Van Vleck propagator and the exact quantum propagator are identical:

$$K(q,q',t) = e^{i\pi D/4} \left(\frac{m}{2\pi\hbar t}\right)^{D/2} \prod_{\mu=1}^{D} \exp\left[\frac{im}{2\hbar t}\left(q_\mu - q'_\mu\right)^2\right] = K_{sc}(q,q',t)$$

This result could have been anticipated because approximate formula (??.37) becomes exact for the free particle Lagrangian.

(Rytis Paškauskas)

Solution 31.19: A usefull determinant identity. *Divide out E in the last column of 31.56 and get the following matrix* ⇓PRELIMINARY

$$E\begin{bmatrix} x_{1,1} & \dots & x_{1,n} & y_1 E^{-1} \\ \vdots & \ddots & \vdots & \vdots \\ x_{n,1} & \dots & x_{n,n} & y_n E^{-1} \\ z_1 & \dots & z_n & 1 \end{bmatrix}$$

Now we subtract the last column multiplied with z_n from the second last column (these matrix operations does not change the determinant) to get

$$E\begin{bmatrix} x_{1,1} & \dots & x_{1,n-1} & x_{1,n} - z_n y_1 E^{-1} & y_1 E^{-1} \\ \vdots & \ddots & \vdots & \vdots & \vdots \\ x_{n,1} & \dots & x_{n,n-1} & x_{n,n} - z_n y_n E^{-1} & y_n E^{-1} \\ z_1 & \dots & z_{n-1} & 0 & 1 \end{bmatrix}$$

This continues eliminating all the z_i's in the bottom row getting the following matrix

$$E\begin{bmatrix} x_{1,1} - z_1 y_1 E^{-1} & \dots & x_{1,n} - z_n y_1 E^{-1} & y_1 E^{-1} \\ \vdots & \ddots & \vdots & \vdots \\ x_{n,1} - z_1 y_n E^{-1} & \dots & x_{n,n} - z_n y_n E^{-1} & y_n E^{-1} \\ 0 & \dots & 0 & 1 \end{bmatrix}$$

and we get (31.57) by expansion from the bottom row.

⇑PRELIMINARY

Chapter 33

Solution 33.1: Monodromy matrix from second variations of the action. *If we take two points in the configuration space q and q' connected with a trajectory with energy E and vary them in such a way that the variation of their initial and final points are transverse to the velocity of the orbit in that point, we can write the variations of the initial and final momenta as*

$$\delta p_{\perp i} = \frac{\partial^2 S(q,q',E)}{\partial q_{\perp i}\partial q_{\perp k}}\delta q_{\perp k} + \frac{\partial^2 S(q,q',E)}{\partial q_{\perp i}\partial q'_{\perp k}}\delta q'_{\perp k} \tag{R.68}$$

and

$$\delta p'_{\perp i} = -\frac{\partial^2 S(q,q',E)}{\partial q'_{\perp i}\partial q_{\perp k}}\delta q_{\perp k} - \frac{\partial^2 S(q,q',E)}{\partial q'_{\perp i}\partial q'_{\perp k}}\delta q'_{\perp k}\,. \tag{R.69}$$

Next we express the variations of the final momenta and coordinates in terms of the initial ones. In the obvious shorthand we can write (R.69) as

$$\delta q_\perp = -S^{-1}_{q'q}S_{q'q'}\delta q'_\perp - S^{-1}_{q'q}\delta p'_\perp,$$

From (R.68) it then follows that

$$\delta p_\perp = (S_{qq'} - S_{qq}S^{-1}_{q'q}S_{q'q'})\delta q'_\perp - S_{qq}S^{-1}_{q'q}\delta p'_\perp. \tag{R.70}$$

These relations remain valid in the $q' \to q$ limit, with q on the periodic orbit, and can also be expressed in terms of the monodromy matrix of the periodic orbit. The monodromy matrix for a surface of section transverse to the orbit within the constant energy $E = H(q,p)$ shell is

$$\begin{aligned}\delta q_\perp &= \mathbf{J}_{qq}\delta q'_\perp + \mathbf{J}_{qp}\delta p'_\perp,\\ \delta p_\perp &= \mathbf{J}_{pq}\delta q'_\perp + \mathbf{J}_{pp}\delta p'_\perp.\end{aligned} \tag{R.71}$$

make into an exercise

In terms of the second derivatives of the action the monodromy matrix is

$$\begin{aligned}\mathbf{J}_{qq} &= -S^{-1}_{q'q}S_{q'q'}\,, & \mathbf{J}_{qp} &= -S^{-1}_{q'q}\,,\\ \mathbf{J}_{pq} &= (S_{qq'} - S_{qq}S^{-1}_{q'q}S_{q'q'})\,, & \mathbf{J}_{pp} &= -S_{qq}S^{-1}_{q'q}\,,\end{aligned}$$

and vice versa

$$\begin{aligned}S_{qq} &= \mathbf{J}_{pp}\mathbf{J}^{-1}_{qp}\,, & S_{qq'} &= \mathbf{J}_{pq} - \mathbf{J}_{pp}\mathbf{J}^{-1}_{qp}\mathbf{J}_{qq},\\ S_{q'q} &= -\mathbf{J}^{-1}_{qp}\,, & S_{q'q'} &= -\mathbf{J}^{-1}_{qp}\mathbf{J}_{qq}.\end{aligned}$$

Now do exercise 33.2.

Solution 33.2: Jacobi gymnastics. *We express the Jacobi matrix elements in*

re full $\det(\mathbf{1}-\mathbf{J})$ $\det(\mathbf{1}-\mathbf{J})$ *with the derivative matrices of* S

e first equation

$$\det(1-J) = \det\begin{pmatrix} I + S_{q'q}^{-1}S_{q'q'} & S_{q'q}^{-1} \\ -S_{qq'} + S_{qq}S_{q'q}^{-1}S_{q'q'} & I + S_{qq}S_{q'q}^{-1} \end{pmatrix}.$$

We can multiply the second column with $S_{q'q'}$ *from the and substract from the first column, leaving the determinant unchanged*

$$\det(1-J) = \det\begin{pmatrix} I & S_{q'q}^{-1} \\ -S_{qq'} - S_{q'q'} & I + S_{qq}S_{q'q}^{-1} \end{pmatrix}.$$

Then, we multiply the second column with $S_{q'q}$ *from the right and compensate this by dividing the determinant with* $\det S_{q'q}$

$$\det(1-J) = \det\begin{pmatrix} I & I \\ -S_{qq'} - S_{q'q'} & S_{q'q} + S_{qq} \end{pmatrix} / \det S_{q'q}.$$

Finally we subtract the first column from the second one

$$\det(1-J_j)) = \det\begin{pmatrix} I & 0 \\ S_{qq'} + S_{q'q'} & S_{qq'} + S_{q'q'} + S_{q'q} + S_{qq} \end{pmatrix} / \det S_{q'q}.$$

The last determinant can now be evaluated and yields the desired result (33.2)

$$\det(1-J_j) = \det(S_{qq'} + S_{q'q'} + S_{q'q} + S_{qq}) / \det S_{q'q}.$$

Chapter 34

Solution 34.1: Evaluation of cycles by minimization. *To start with a guess path where each bounce is given some arbitrary position on the correct disk and then iteratively improve on the guess. To accomplish this an improvement cycle is constructed whereby each bouncing point in the orbit is taken in turn and placed in a new position so that it minimizes the path. Since the positions of all the other bounces are kept constant this involves choosing the new bounce position which minimizes the path from the previous bounce to the next bounce. This problem is schematically represented in figure R.12*

Finding the point B *involves a one dimensional minimization. We define the vectors* $\vec{A} = \vec{OA}$, $\vec{B} = \vec{OB}$ *and* $\vec{C} = \vec{OC}$. *We wish to minimize the length* L_{ABC} *by varying* $\vec{B}$ *subject to the constraint that* $|\vec{B}| = a$. *Clearly*

$$\begin{aligned} L_{ABC} &= \left|\vec{A} - \vec{B}\right| + \left|\vec{C} - \vec{B}\right| \\ &= \sqrt{\vec{A}^2 + \vec{B}^2 - 2\vec{A}\cdot\vec{B}} + \sqrt{\vec{C}^2 + \vec{B}^2 - 2\vec{C}\cdot\vec{B}} \end{aligned}$$

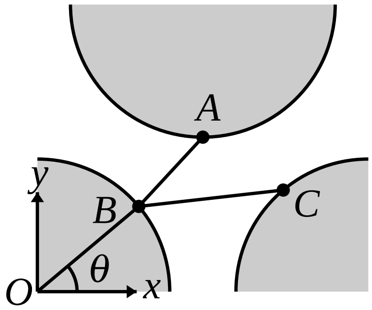

Figure R.12: Minimizing the path from the previous bounce to the next bounce.

writing

$$\vec{B}(\theta) = a(\cos\theta, \sin\theta)$$

then the minima is given by

$$\frac{dL_{ABC}}{d\theta} = -\left(\frac{\vec{A}}{\sqrt{\vec{A}^2 + \vec{B}^2 - 2\vec{A}\cdot\vec{B}}} + \frac{\vec{C}}{\sqrt{\vec{C}^2 + \vec{B}^2 - 2\vec{C}\cdot\vec{B}}} \right) \cdot \vec{B}'(\theta) = 0.$$

The minima can then be found using a bisection algorithm or using Newton-Raphson. A simpler way is to observe that $\vec{B}'(\theta)$ is orthogonal to $\vec{B}(\theta)$ so that the vector

$$\vec{D} = \frac{\vec{A}}{\sqrt{\vec{A}^2 + \vec{B}^2 - 2\vec{A}\cdot\vec{B}}} + \frac{\vec{C}}{\sqrt{\vec{C}^2 + \vec{B}^2 - 2\vec{C}\cdot\vec{B}}}$$

will be proportional to $\vec{B}$. This then provides an iterative sequence for finding $\vec{B}$

- *Starting from your current guess for $\vec{B}$ calculate $\vec{D}$*
- *Put $\vec{B} = a\vec{D}/|\vec{D}|$*
- *Repeat the first step until you converge.*

At each iteration of the improvement cycle the total length of the orbit is measured. The minimization is complete when the path length stops improving. Although this algorithm is not as fast as the Newton-Raphson method, it nevertheless converges very rapidly.

(Adam Prügel-Bennet)

Chapter 35

Solution 35.2: The one-disk scattering wave function.

$$\psi(\vec{r}) = \frac{1}{2}\sum_{m=-\infty}^{\infty} \left(H_m^{(2)}(kr) - \frac{H_m^{(2)}(ka)}{H_m^{(1)}(ka)} H_m^{(1)}(kr) \right) e^{im(\Phi_r - \Phi_k)} . \qquad \text{(R.72)}$$

(For $r < a$, $\psi(\vec{r}) = 0$ of course.)

(Andreas Wirzba)

ELIMINARY

Solution 35.5: Ghosts do not exist. *In ref. [M.1] the ghost cancellation rule (**??**) is proved for the convolution of two $\mathbf{A}$-matrices and generalized to hold also inside an arbitrary (periodic) itinerary (with and without creeping sections).*

Consider the itinerary $(1, \underline{2}, 3, 4, \underline{5}, 6)$ with ghost sections at disk 2 and 5 resulting from the sixth order trace. Its geometrical contribution cancels in the trace-log expansion against the geometrical reduction of the itineraries $(1, \underline{2}, 3, 4, 6)$, $(1, 3, 4, \underline{5}, 6)$ from the 5th-order trace with ghost sections at disk 2 or 5, respectively, and against the geometrical reduction of the itinerary $(1, 3, 4, 6)$ of the 4th-order trace with no ghost contribution:

$$
\begin{aligned}
&-\frac{1}{6}\left(6\,\underline{\mathbf{A}}^{1,\underline{2}}\underline{\mathbf{A}}^{\underline{2},3}\mathbf{A}^{3,4}\underline{\mathbf{A}}^{4,\underline{5}}\underline{\mathbf{A}}^{\underline{5},6}\mathbf{A}^{6,1}\right)\\
&\qquad-\frac{1}{5}\left(5\,\underline{\mathbf{A}}^{1,\underline{2}}\underline{\mathbf{A}}^{\underline{2},3}\mathbf{A}^{3,4}\mathbf{A}^{4,6}\mathbf{A}^{6,1}+5\,\mathbf{A}^{1,3}\mathbf{A}^{3,4}\underline{\mathbf{A}}^{4,\underline{5}}\underline{\mathbf{A}}^{\underline{5},6}\mathbf{A}^{6,1}\right)\\
&\qquad-\frac{1}{4}\left(4\,\mathbf{A}^{1,3}\mathbf{A}^{3,4}\mathbf{A}^{4,6}\mathbf{A}^{6,1}\right)\\
&= \quad (-1+2-1)\,\mathbf{A}^{1,3}\mathbf{A}^{3,4}\mathbf{A}^{4,6}\mathbf{A}^{6,1} = 0\,.
\end{aligned}
$$

*The prefactors $-1/4$, $-1/5$, $-1/6$ result from the trace-log expansion, the factors 4, 5, 6 inside the brackets are due to the cyclic permutations, and the rule (**??**) was used. If there are two or more ghost segments adjacent to each other, the ghost rule (**??**) has to be generalized to*

$$
\begin{aligned}
&\cdots\underline{\mathbf{A}}^{i,\underline{i+1}}\underline{\mathbf{A}}^{\underline{i+1},\underline{i+2}}\cdots\underline{\mathbf{A}}^{\underline{i+k},\underline{i+k+1}}\cdots\underline{\mathbf{A}}^{\underline{i+n-1},i+n}\cdots\\
&= \quad \cdots\left(-\underline{\mathbf{A}}^{i,\underline{i+2}}\right)\cdots\underline{\mathbf{A}}^{\underline{i+k},\underline{i+k+1}}\cdots\underline{\mathbf{A}}^{\underline{i+n-1},i+n}\cdots\\
&= \quad \cdots\underline{\mathbf{A}}^{i,\underline{i+3}}\cdots\underline{\mathbf{A}}^{\underline{i+k},\underline{i+k+1}}\cdots\underline{\mathbf{A}}^{\underline{i+n-1},i+n}\cdots\\
&= \quad \cdots(-1)^{n-1}\mathbf{A}^{i,i+n}\cdots\,. \qquad\qquad (R.73)
\end{aligned}
$$

Finally, let us discuss one case with a repeat, e.g. the itinerary $(1, \underline{2}, 3, 4, 1, \underline{2}, 3, 4)$ with repeated ghost sections at disk 2 in the semiclassical limit. The cancellations proceed in the trace-log expansion as follows:

$$
\begin{aligned}
&-\frac{1}{8}\left(4\,\underline{\mathbf{A}}^{1,\underline{2}}\underline{\mathbf{A}}^{\underline{2},3}\mathbf{A}^{3,4}\mathbf{A}^{4,1}\underline{\mathbf{A}}^{1,\underline{2}}\underline{\mathbf{A}}^{\underline{2},3}\mathbf{A}^{3,4}\mathbf{A}^{4,1}\right)\\
&\qquad-\frac{1}{7}\left(7\,\underline{\mathbf{A}}^{1,\underline{2}}\underline{\mathbf{A}}^{\underline{2},3}\mathbf{A}^{3,4}\mathbf{A}^{4,1}\mathbf{A}^{1,3}\mathbf{A}^{3,4}\mathbf{A}^{4,1}\right)\\
&\qquad-\frac{1}{6}\left(3\,\mathbf{A}^{1,3}\mathbf{A}^{3,4}\mathbf{A}^{4,1}\mathbf{A}^{1,3}\mathbf{A}^{3,4}\mathbf{A}^{4,1}\right)\\
&= \quad \left(-\frac{1}{2}+1-\frac{1}{2}\right)\left[\mathbf{A}^{1,3}\mathbf{A}^{3,4}\mathbf{A}^{4,1}\right]^2 = 0
\end{aligned}
$$

Note that the cyclic permutation factors of the 8th and 6th order trace are halved because of the repeat. The occurrence of the ghost segment in the second part of the 7th order itinerary is taken care of by the weight factor 7.

(Andreas Wirzba)

⇑PRELIMINARY
⇓PRIVATE

uniform approximation

Chapter 37

⇑PRIVATE

(No solutions available.)

Chapter 38

(No solutions available.)

Chapter 40

⇓PRIVATE

(No solutions available.)

Chapter 41

create more exercises...

Solution 41.1: Symmetric cusp catastrophe. *The cusp catastrophe is described by the normal form (41.4)*

$$\Phi_a(x) = \frac{1}{4}x^4 - \frac{1}{2}ax^2 \,.$$

It has stationary points for $t = 0$ and $t = \pm\sqrt{a}$. From (41.23) we have

$$S_2(E) = S_0(E) - \frac{1}{4}a^2 \,, \qquad S_1(E) = S_0(E) \,,$$

since $\Phi_a(0) = 0$. It follows that

$$\Delta S = S_1 - S_2 = a^2/4 \,, \qquad a = \pm 2\sqrt{\Delta S} \,.$$

In case $S_2 > S_1$, we need to replace the catastrophe (41.4) with its negative and proceed at the same way. Let now $\mathcal{A}_2$ be the sum of the amplitudes of the pair of orbits born in the bifurcation for $a > 0$, and $\mathcal{A}_1$ the amplitude of the single orbit corresponding to the $x = 0$ stationary point of the normal form. Given the reflection symmetry, we can write the $p(x)$ in (41.21) as

$$p(x) = p_0 + p_2 x^2 \,.$$

Now, from the asymptotic expression (41.22) it follows in general that

$$\mathcal{A}_i = p(x_i)\, \frac{(2\pi i)^{n/2}}{\sqrt{|\Phi_a''(x_i)|}}\, e^{-i\pi\nu_i/2} \,,$$

from which in our case we get

$$p_0 = \sqrt{\frac{a}{2\pi}}\mathcal{A}_1 e^{i\pi/4}\,, \qquad p_2 = \frac{e^{-i\pi/4}}{2\sqrt{\pi a}}\left(\mathcal{A}_2 - \sqrt{2}i\mathcal{A}_1\right)\,. \tag{R.74}$$

According to the ansatz (41.20), the uniform approximation takes the form (41.7):

$$\Psi(E) = p_0 \int dx\, e^{i(\frac{1}{4}x^4 - \frac{1}{2}ax^2)} + p_2 \int dx\, x^2 e^{i(\frac{1}{4}x^4 - \frac{1}{2}ax^2)}\,,$$

of which the first integral is (41.8)

$$\frac{\pi}{2}\sqrt{|a|}e^{-ia^2/8}\left[e^{i\pi/8}J_{-1/4}\left(\frac{a^2}{8}\right) + sign(a)e^{-i\pi/8}J_{-1/4}\left(\frac{a^2}{8}\right)\right]\,,$$

fix Bessel subscripts

and the other is just

$$I_2 = 2i\frac{dI_0}{da}\,.$$

(Domenico Lippolis)

⇑PRIVATE

Chapter E

(No solutions available.)

Chapter F

(No solutions available.)

Chapter G

Solution G.1: Lefschetz zeta function. *Starting with dynamical zeta function ref. [13.11] develops the Atiyah-Bott-Lefschetz fixed point formula and relates is to Weyl characters. Might be worth learning.*

Chapter I

Solution I.1: *Using the multiplicative property of the Jacobi matrix we can write*

$$\Lambda^{t'+t}(x_0, \mathbf{u}_0) = ||\mathbf{J}^{t'+t}(x_0)\mathbf{u}_0|| = ||\mathbf{J}^{t'}(x(t))\mathbf{J}^t(x_0)\mathbf{u}_0||.$$

We can introduce the time evolved unit vector

$$\mathbf{u}(t) = \mathbf{J}^t(x_0)\mathbf{u}_0/||\mathbf{J}^t(x_0)\mathbf{u}_0||.$$

Then

$$||\mathbf{J}^{t'}(x(t))\mathbf{J}^t(x_0)\mathbf{u}_0|| = ||\mathbf{J}^{t'}(x(t))\mathbf{u}(t)||||\mathbf{J}^t(x_0)\mathbf{u}_0||,$$

which is the desired result.

We have to adjoin the tangent space, since the stretching factor depends on $\mathbf{u}$ *and not just on* x. *The stretching factor is multiplicative along the entire trajectory* $(x(t), \mathbf{u}(t))$. *However, it is not multiplicative along the phase space trajectory* $x(t)$ *with a fixed* $\mathbf{u}$.

Solution I.2: *If* $b = a^2$ *and* $T_b = 2T_a$ *we can introduce the variable* $y = e^{sT_a}$. *The dynamo rate equation then reads*

$$0 = 1 - x + x^2.$$

The solutions of this are $x_\pm = (1 \pm i\sqrt{3})/2$. *The dynamo rate is then a complex cojugate pair* $\nu = \log x_\pm/T_a$.

The escape rate equation is

$$0 = 1 - x/a - x^2/a^2.$$

The solutions are $x_\pm = a(-1 \pm \sqrt{5})/2$. *The escape rate is* $\gamma = \log(x_+)/T_a$.

In the reverse case the escape rate remains unchanged, while the dynamo rate becomes $\nu = \log((\sqrt{5}+1)/2)/T_a$. *In this case the advected field grows with an exponential rate. In the previous case it shows oscillations in addition to the exponential growth due to the imaginary part of the rate.*

⇓PRIVATE

Chapter L

(No solutions available.)

⇑PRIVATE

Chapter N

(No solutions available.)